

Search for CP violating anomalous top quark coupling in pp collisions at $\sqrt{s} = 13$ TeV (CMS-PAS-TOP-18-007)

Seungkyu Ha (Yonsei University)

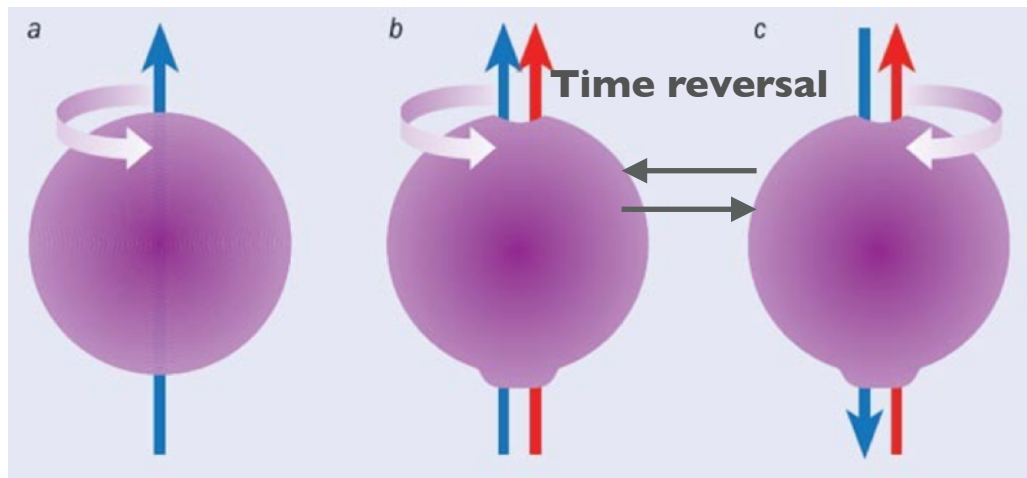
on behalf of the CMS Collaboration

Nov. 23, 2020

CMS Highlight @ LHC-TOP-WG Meeting

Introduction

- CP violation (CPV) is a candidate to explain the matter-antimatter but it has not been observed beyond the expectation of the SM
- In the SM, CPV in the production and decay of top quark pairs is predicted to be very small
- Search the new source of CPV using top quark pair events in the **dilepton channels**; chromoelectric dipole moment, **CEDM**



↑ : Magnetic Dipole Moment

↑ : Electric Dipole Moment

$$\mathcal{L} = \frac{g_s}{2} \bar{t} T^a \sigma^{\mu\nu} (a_t^g + i\gamma_5 d_t^g) t G_{\mu\nu}^a$$

d_t^g is CEDM

- Physics Observable :

-Theory paper: [10.1103/PhysRevD.93.014020](https://arxiv.org/abs/10.1103/PhysRevD.93.014020)

$$\mathcal{O}_1 = \epsilon(p_t, p_{\bar{t}}, p_{l^+}, p_{l^-}) = \begin{vmatrix} E_t & p_{tx} & p_{ty} & p_{tz} \\ E_{\bar{t}} & p_{\bar{t}x} & p_{\bar{t}y} & p_{\bar{t}z} \\ E_{l^+} & p_{l^+x} & p_{l^+y} & p_{l^+z} \\ E_{l^-} & p_{l^-x} & p_{l^-y} & p_{l^-z} \end{vmatrix}$$

$$\mathcal{O}_3 = \epsilon(p_b, p_{\bar{b}}, p_{l^+}, p_{l^-}) = \begin{vmatrix} E_b & p_{bx} & p_{by} & p_{bz} \\ E_{\bar{b}} & p_{\bar{b}x} & p_{\bar{b}y} & p_{\bar{b}z} \\ E_{l^+} & p_{l^+x} & p_{l^+y} & p_{l^+z} \\ E_{l^-} & p_{l^-x} & p_{l^-y} & p_{l^-z} \end{vmatrix}$$

- These physics observables have CP-odd correlation, and allow us to test CP violation in top-quark pair events

- Asymmetries :

$$A_i \equiv \frac{N_{events}(\mathcal{O}_i > 0) - N_{events}(\mathcal{O}_i < 0)}{N_{events}(\mathcal{O}_i > 0) + N_{events}(\mathcal{O}_i < 0)} \quad i = 1 \text{ or } 3$$

- Allow to infer the CEDM of top quark (linearly correlated)

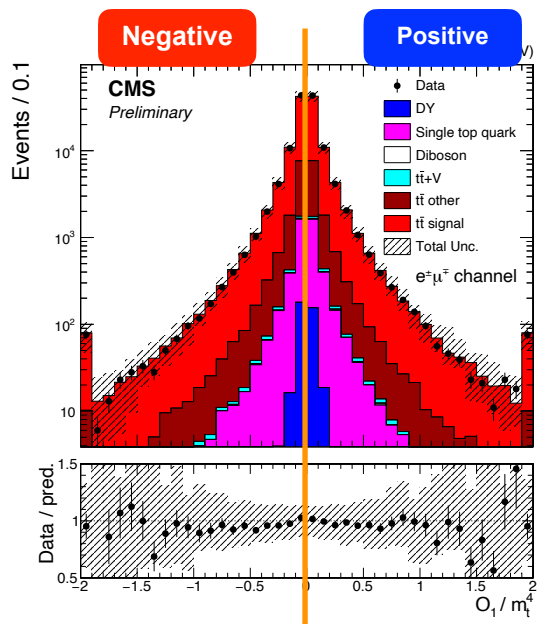
Analysis Procedure

- **The main goal of this analysis**

Extraction the asymmetry and CEDM in top pair events in the dilepton final state

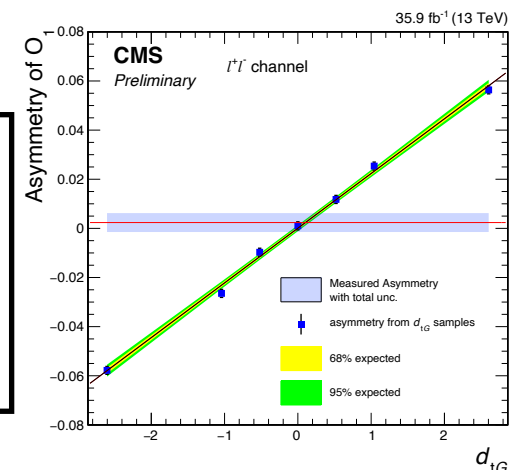
CMS 2016 data set, 35.9 fb⁻¹

- Selection of events top pair events in the dilepton final state
- DY contribution estimated (Rout/in)
- Reconstruction of top quarks
- Calculate O1 and O3



Extraction of Asymmetry of O1 & O3 Using a maximum likelihood fit

Extraction of CEDM Using the generated CP-violation events



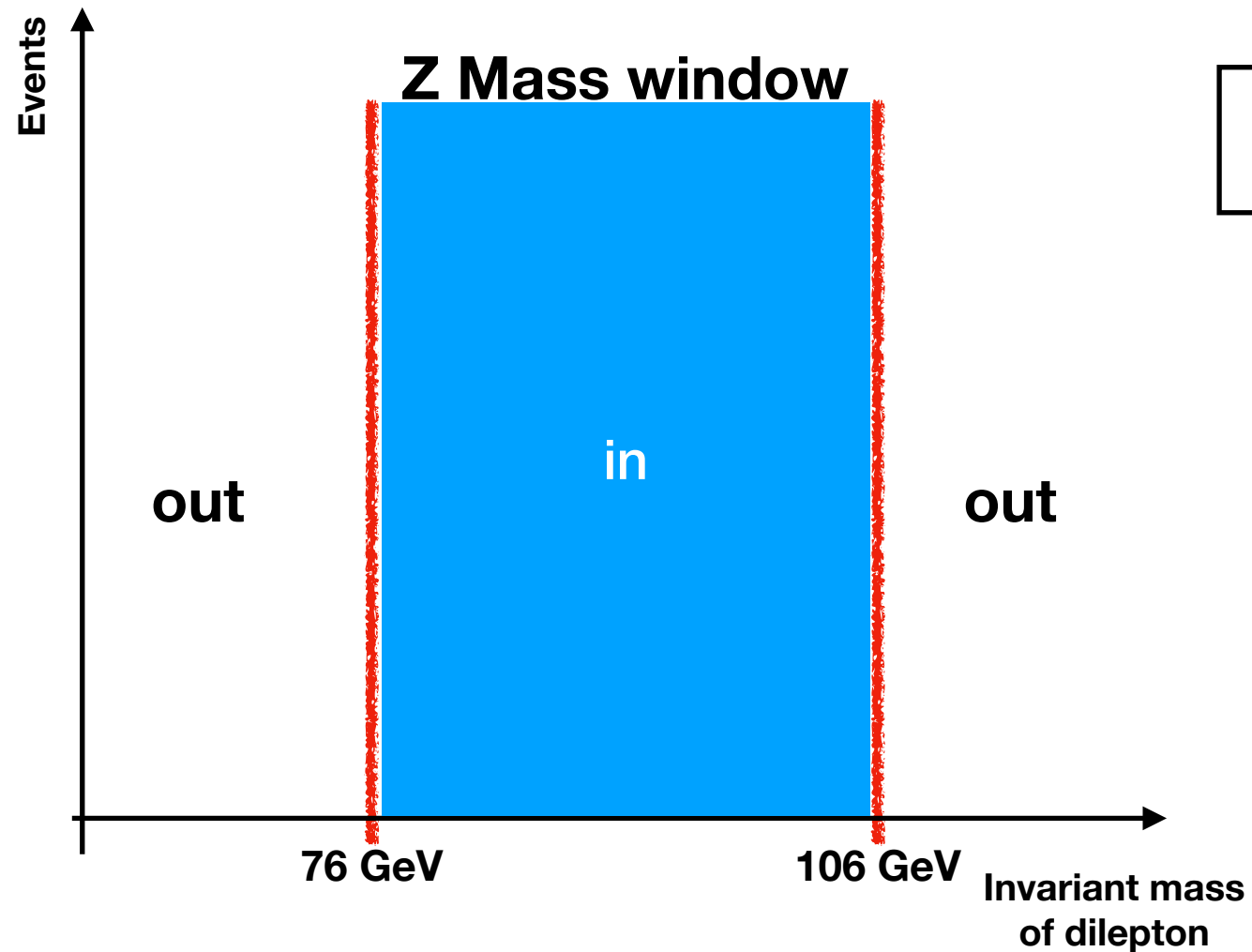
- Object Selection**

Requirement	Muon	Electron	Jet
ID & Isolation	Tight ID PFIso < 0.15 (Tight)	Tight (Cut Based)	PF Loose
Kinematic Requirement	η < 2.4 Leading lepton $p_T > 25$ GeV & Sub-leading Lepton $p_T > 20$ GeV		$p_T > 30$ GeV, η < 2.4
b-tagging	-		Medium (CSVv2)

- Event Selection**

Cut flow	Dimuon & Dielectron	Muon-electron
Trigger & MET filters	0	0
Lepton requirement & $M_{ll} > 20$ GeV & Third lepton veto	0	0
Z mass veto (76 GeV < M_{ll} < 106 GeV)	0	-
Num. of Jet ≥ 2	0	0
MET > 40 GeV	0	-
Num. b-tagged Jet ≥ 1 (CSVv2, Medium W.P.)	0	0
Top reconstruction (Kinematic solver)	0	0

- To determine DY background, we follow the method ($R_{out/in}$) suggested in [1,2,3].



$$N_{out}^{l^+l^-,data} = R_{out/in}^{l^+l^-} (N_{in}^{l^+l^-,data} - 0.5 \cdot k_{ll} \cdot N_{in}^{e\mu,data})$$

where $ll = \mu\mu$ or ee , $R_{out/in} = \frac{N_{DY MC}^{out}}{N_{DY MC}^{in}}$

for k_{ll} , $k_{ee} = \sqrt{\frac{N_{in}^{e^+e^-}}{N_{out}^{\mu^+\mu^-}}}$, $k_{\mu\mu} = \sqrt{\frac{N_{in}^{\mu^+\mu^-}}{N_{out}^{e^+e^-}}}$

	$\mu^+\mu^-$	e^+e^-	$e^\pm\mu^\mp$
SF	1.1	1.1	1.2

[1] E. P. J. Cuevas, J. R. Gonzalez, "Measurement of the Top-Quark Pair Production Cross Section in the Dilepton Channel with 35.9 fb⁻¹ of 13 TeV data using the Cut and Count Method", CMS Note 2017/039, 2017
 [2] W. Andrews and et al., "A Method to Measure the Contribution of DY → l+l- to a di-lepton + MET Selection", CMS Note 2009/023, 2009.
 [3] S. Chenarani and et al., "Measurement of the cross-section for tW production in dilepton final states at 13 TeV using 2016 data", CMS Note 2017/132, 2017.

kinematic reconstruction

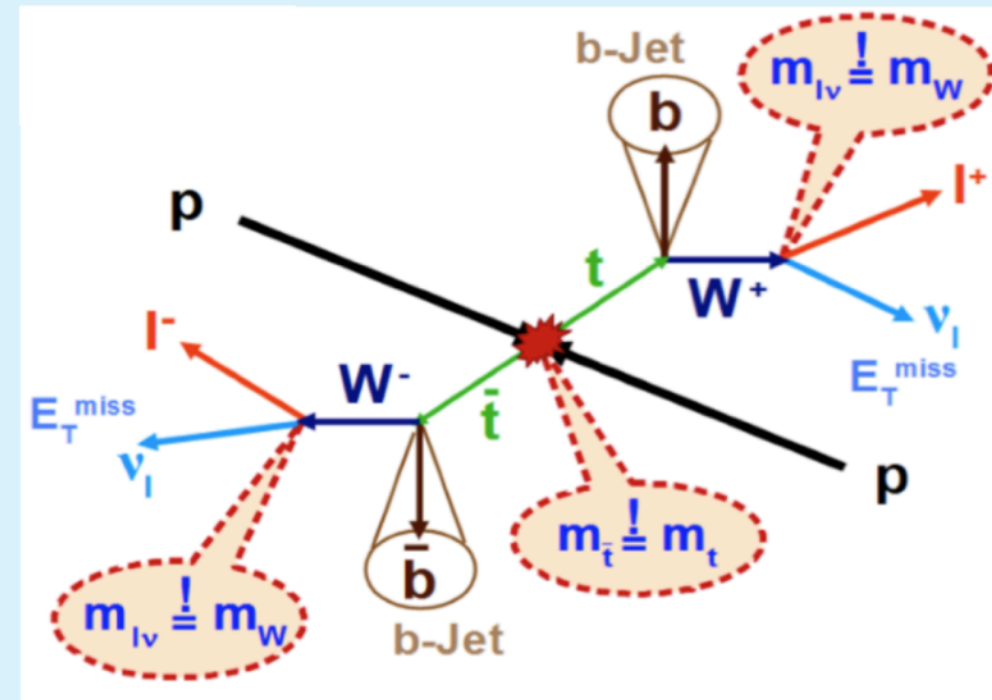
inputs: 2 jets, 2 leptons, MET

constraints:

- $m_t, m_{t\bar{t}}$ → 2
- m_{W^+}, m_{W^-} → 2
- $P_T(\vec{\nu} + \vec{\bar{\nu}}) = MET$ → 2

unknowns:

$\vec{\nu}, \vec{\bar{\nu}} \rightarrow 6$



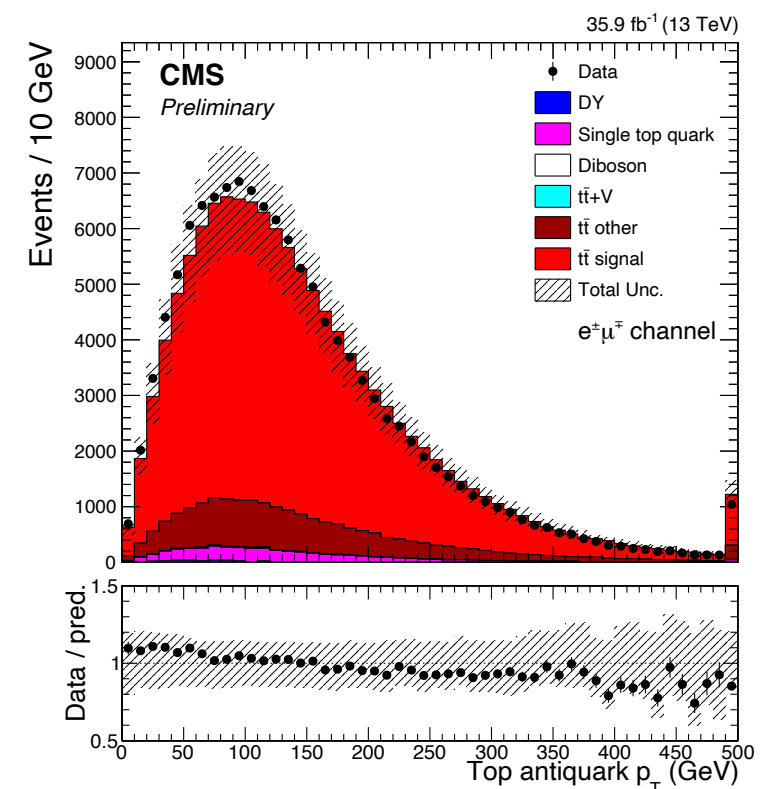
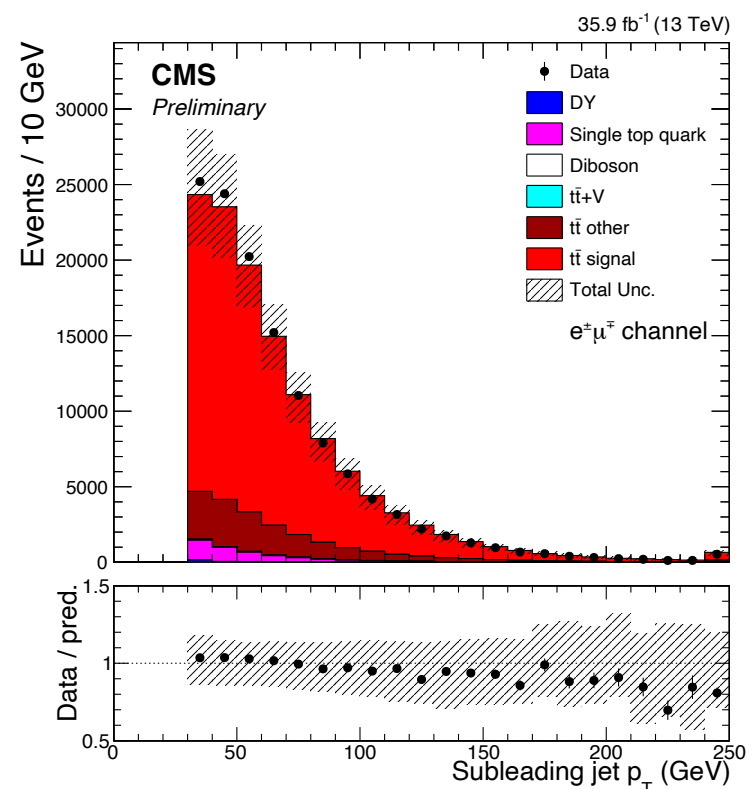
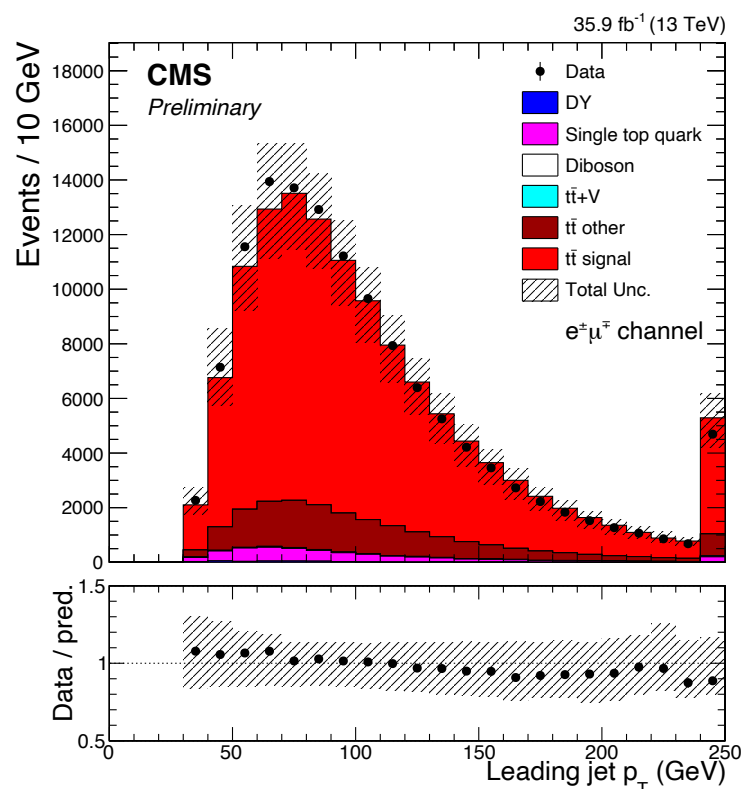
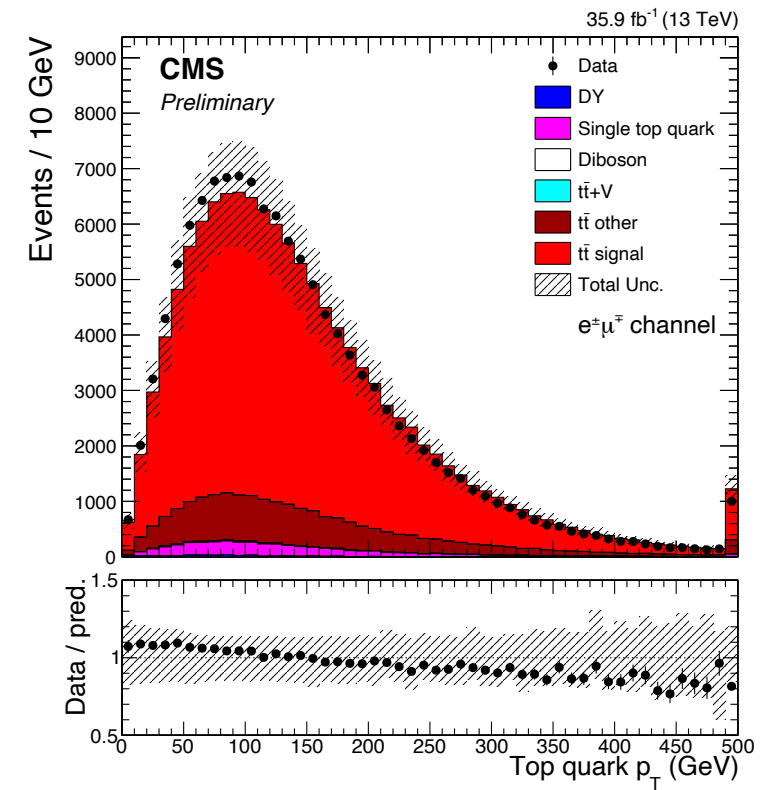
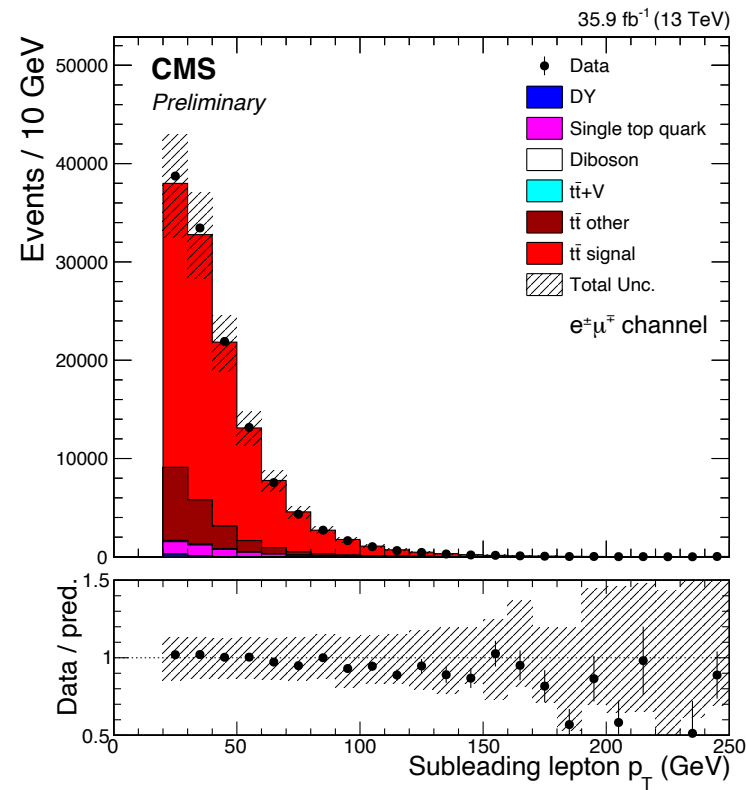
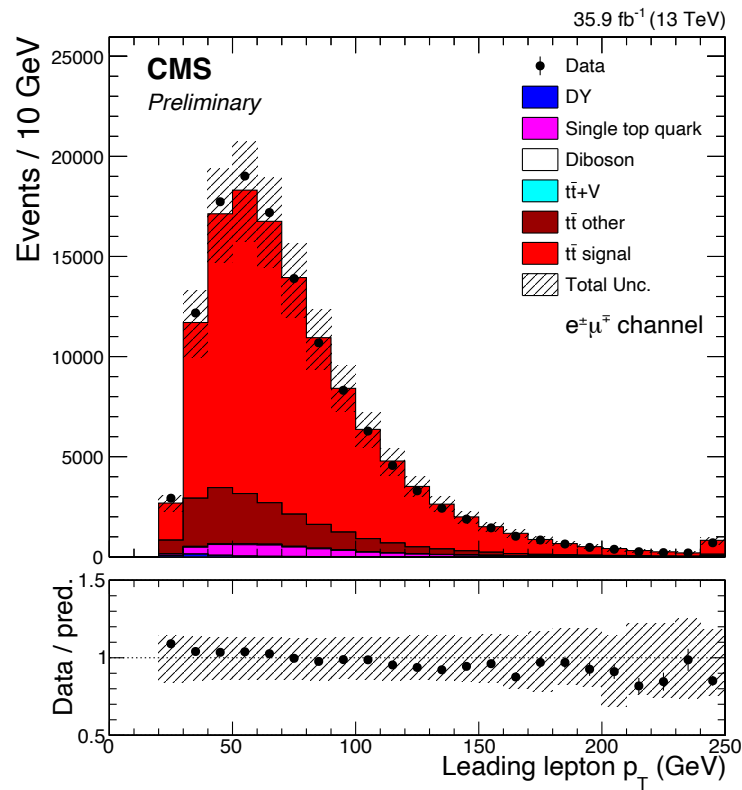
- reconstruct event 100 times and smear inputs by their resolution:
 - top mass fixed to 172.5 GeV
 - w mass smeared according to gen-level W mass distribution
 - take weighted average of solutions for all smearings
 - weights defined according to gen-level m_{lb} distribution

$$p_{x,y,z}^{top} = \frac{1}{W} \sum_{i=0}^{100} w_i \cdot (p_{x,y,z}^{top})_i$$

20/03/18

Slide courtesy by Mykola Savitskyi

- p_T distribution of leading leptons, jets and top quarks



Event Yield

- Simulated and observed event yields with their statistical uncertainties for the three dilepton channels.

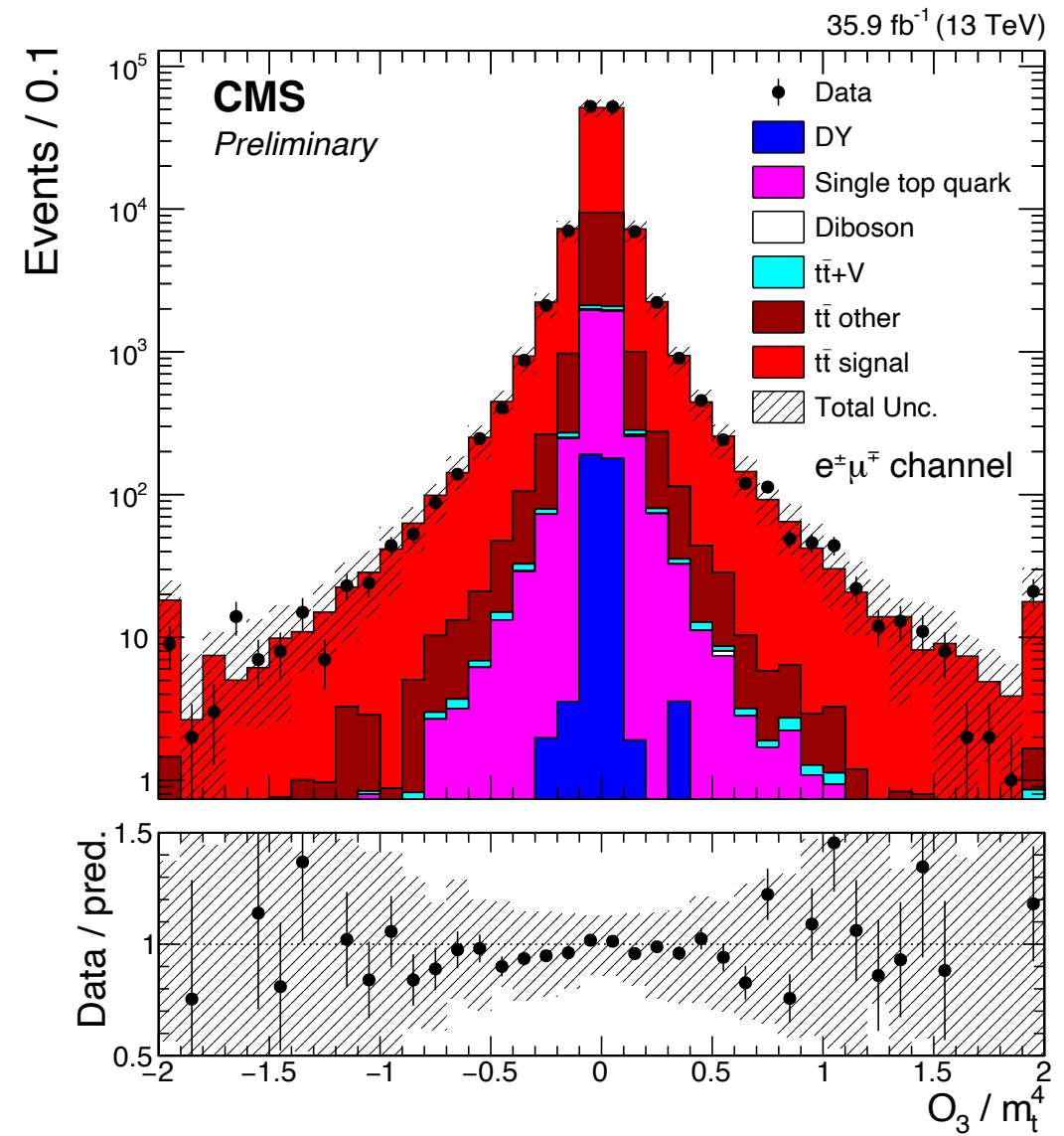
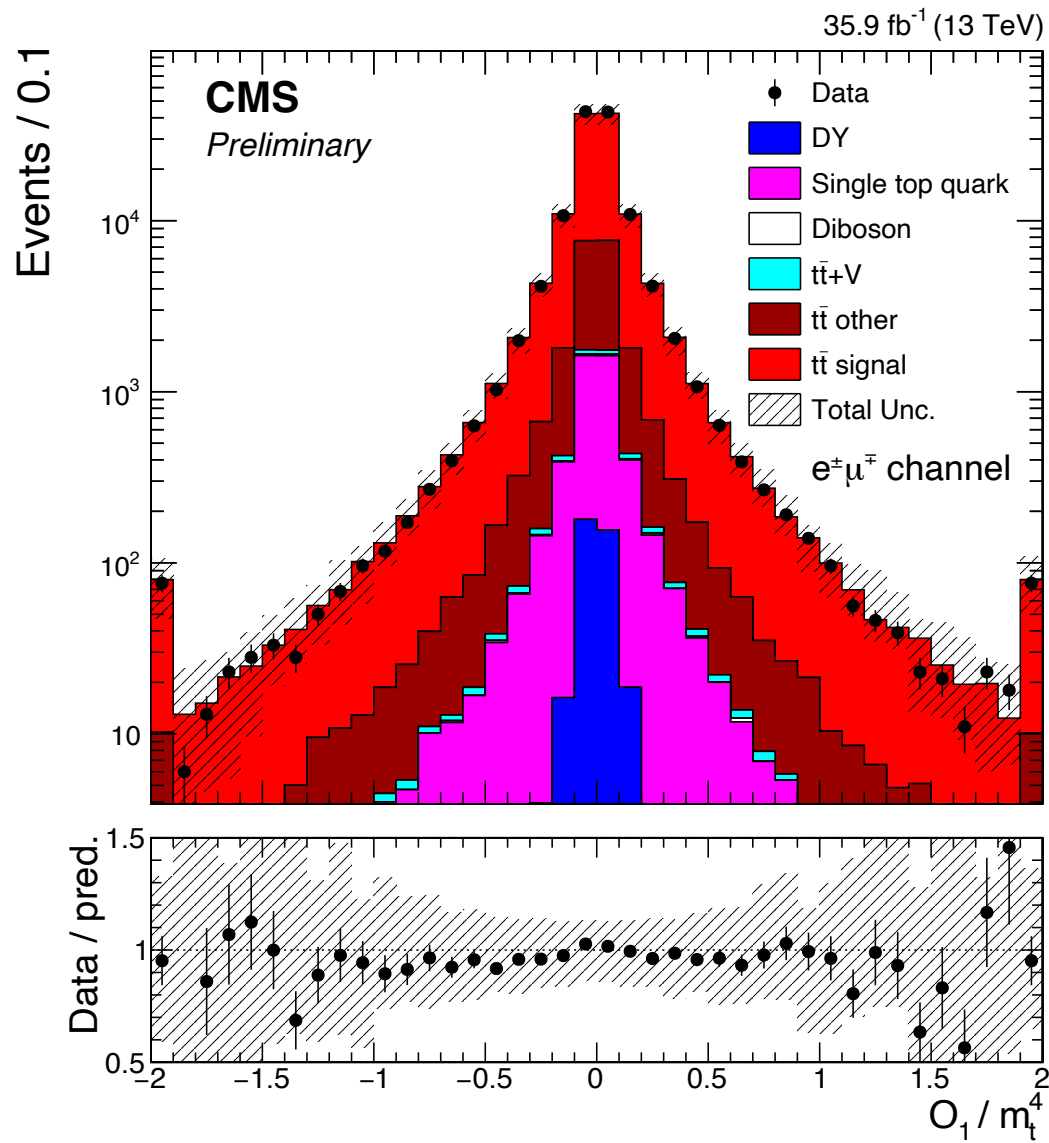
- **Only statistical uncertainty**

Process	$\mu^+\mu^-$	e^+e^-	$e^\pm\mu^\mp$
DY	1627 \pm 95	700 \pm 57	381 \pm 26
Single top quark	1793 \pm 18	899 \pm 13	4265 \pm 28
$t\bar{t}+V$	144 \pm 3	72 \pm 2	302 \pm 4
Diboson	70 \pm 6	37 \pm 4	100 \pm 7
$t\bar{t}$ other	7502 \pm 38	3425 \pm 25	16787 \pm 56
$t\bar{t}$ signal	45818 \pm 93	22216 \pm 64	104051 \pm 140
Total prediction	56954 \pm 140	27350 \pm 90	125878 \pm 155
Observed data	55993	26961	126549

- The discrepancy between observed and simulated events is lower than $\sim 3\%$.
 ($\mu^+\mu^-$: $\sim 3\%$, e^+e^- : $\sim 2.9\%$, $e^\pm\mu^\mp$: $\sim 0.8\%$)

Distribution of O_1 and O_3 ($e^\pm \mu^\mp$)

- Distribution of O_1 and O_3



We extracted asymmetries with maximum likelihood fit

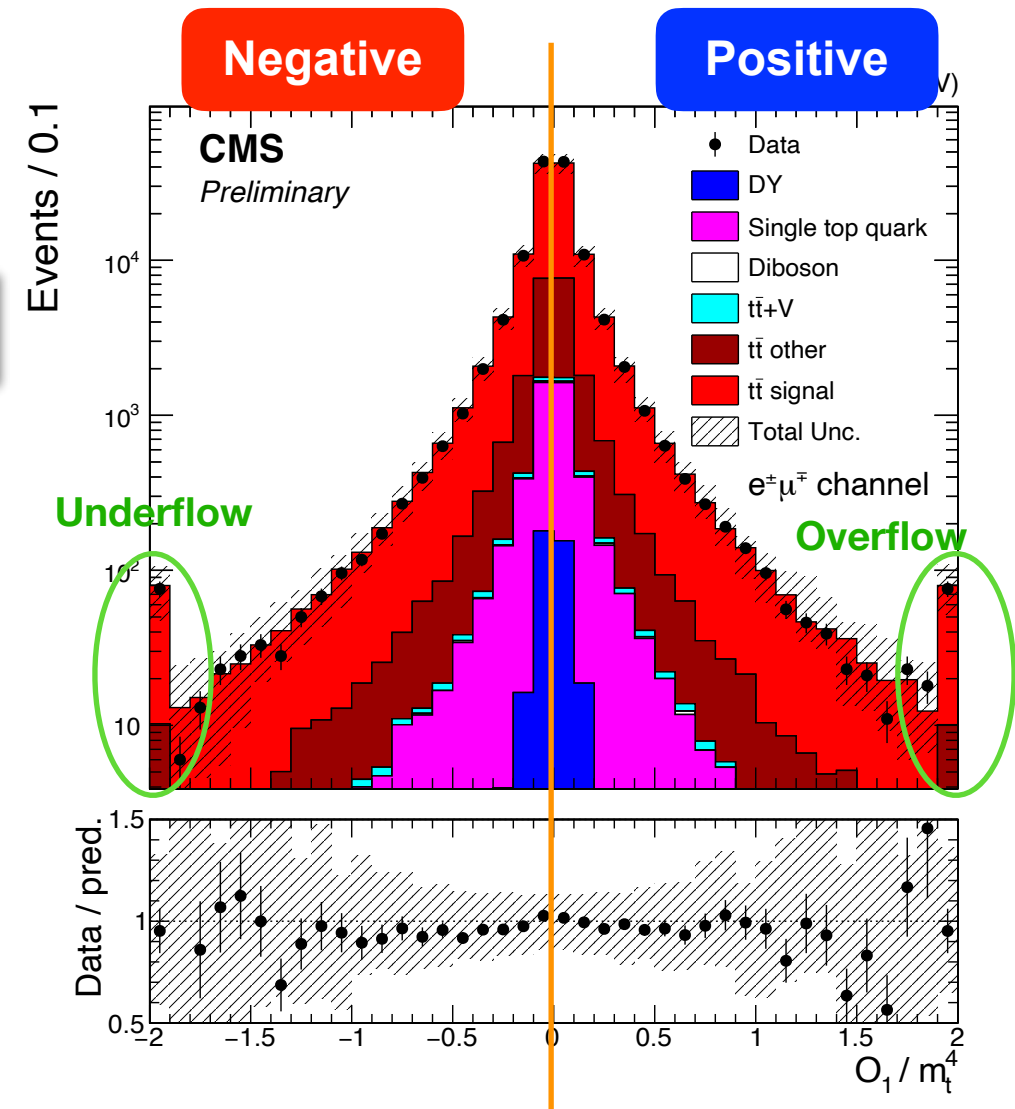
- Definition of the likelihood fit function

$$\mathcal{L}(A_i, \sigma_{t\bar{t}}) = \mathcal{P}(N_+^{\text{obs}}, N_+^{\text{pred}}) \cdot \mathcal{P}(N_-^{\text{obs}}, N_-^{\text{pred}})$$

$$N_{\pm}^{\text{pred}} = N^{t\bar{t}} \frac{1 \pm A_i}{2} + N^{\text{bkg}} f_{\pm}^{\text{bkg}},$$

$$N^{t\bar{t}} = L \cdot \mathcal{B} \cdot \epsilon_{\text{sig}} \cdot \sigma_{t\bar{t}}$$

made A and x-section float



- By minimizing the negative log-likelihood function, we extract asymmetry

Sources of Systematic Uncertainties

- Basically, we considered two types of systematic uncertainties

Experimental uncertainties	Modeling uncertainties
Luminosity uncertainty	Parton distribution function
Pileup reweighting	Factorization & Renormalization
Jet energy scale uncertainty	ME-PS matching scale
Jet energy resolution uncertainty	Color reconnection
Muon momentum correction	Top p_T reweighting
Electron energy scale and smearing	b-fragmentation
Lepton ID and isolation scale factors	Semileptonic branching ratio of b hadron
Unclustered energy of MET	Hadronization model
b-quark jet tag scale factor	ISR
Limited statistics of background (BG) models	FSR
Jet ϕ Resolution	Underlying event
Charge Mis identification (Leptons)	Top mass
Different response of b/b-bar quark jet	-

Additional systematic uncertainty sources (next slide)

- Dilution factor is important in our analysis. Physics observables to test CP violation are the **determinant of 4X4 Matrix** which consists of 4-vectors of top quarks, b-quark jets and leptons.

If either the 4-vectors or the order of component of determinant(\mathcal{O}_i) is changed, the sign of the physics observable \mathcal{O}_i is also changed. So it will affect the asymmetry.

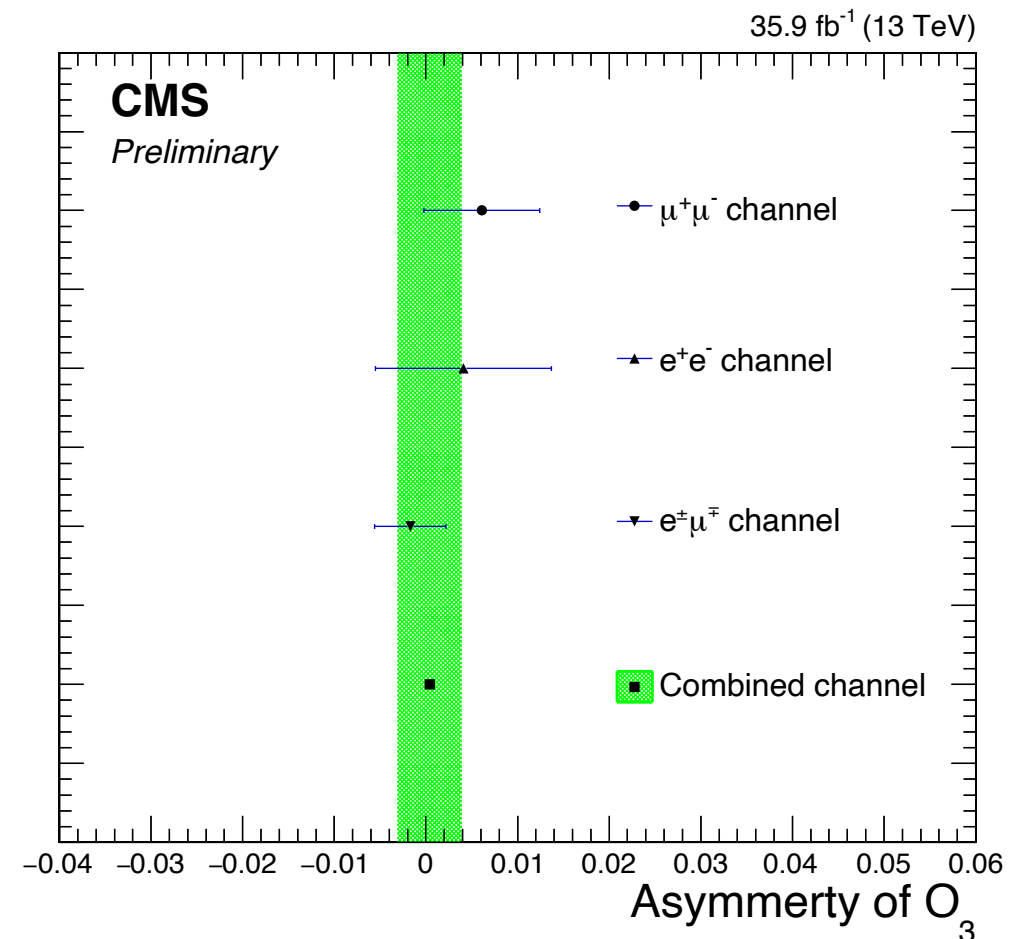
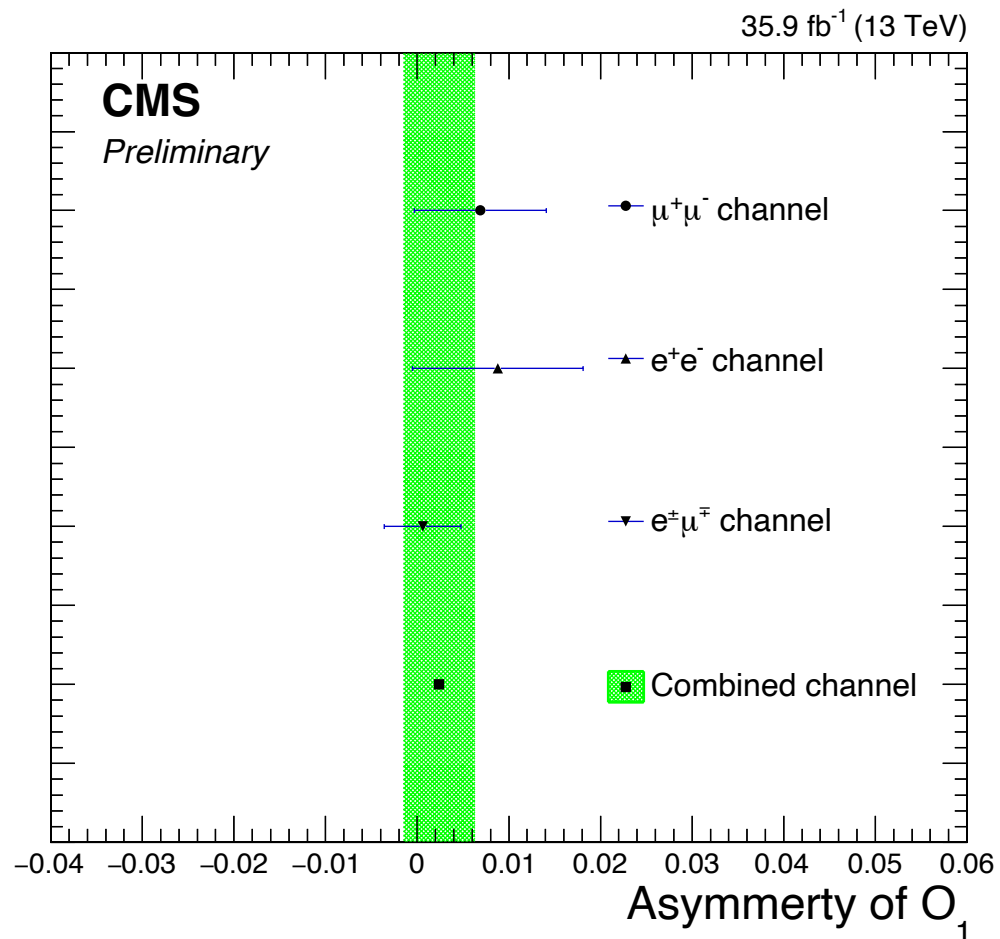
$$\mathcal{O}_1 = \epsilon(p_t, p_{\bar{t}}, p_{l+}, p_{l-})$$

$$\mathcal{O}_3 = \epsilon(p_b, p_{\bar{b}}, p_{l+}, p_{l-})$$

$$A_i \equiv \frac{N_{events}(\mathcal{O}_i > 0) - N_{events}(\mathcal{O}_i < 0)}{N_{events}(\mathcal{O}_i > 0) + N_{events}(\mathcal{O}_i < 0)}$$

- Jet ϕ Resolution (Angular Resolution)
 - Shifted phi of jets by ϕ Resolution
- Charge Mis-Identification
 - One lepton charge mis-identification
 - Two lepton charge mis-identification
- b & b-bar quark Jet Different Response
 - Applied b& b-bar quark jet difference to MC simulation

- Asymmetry

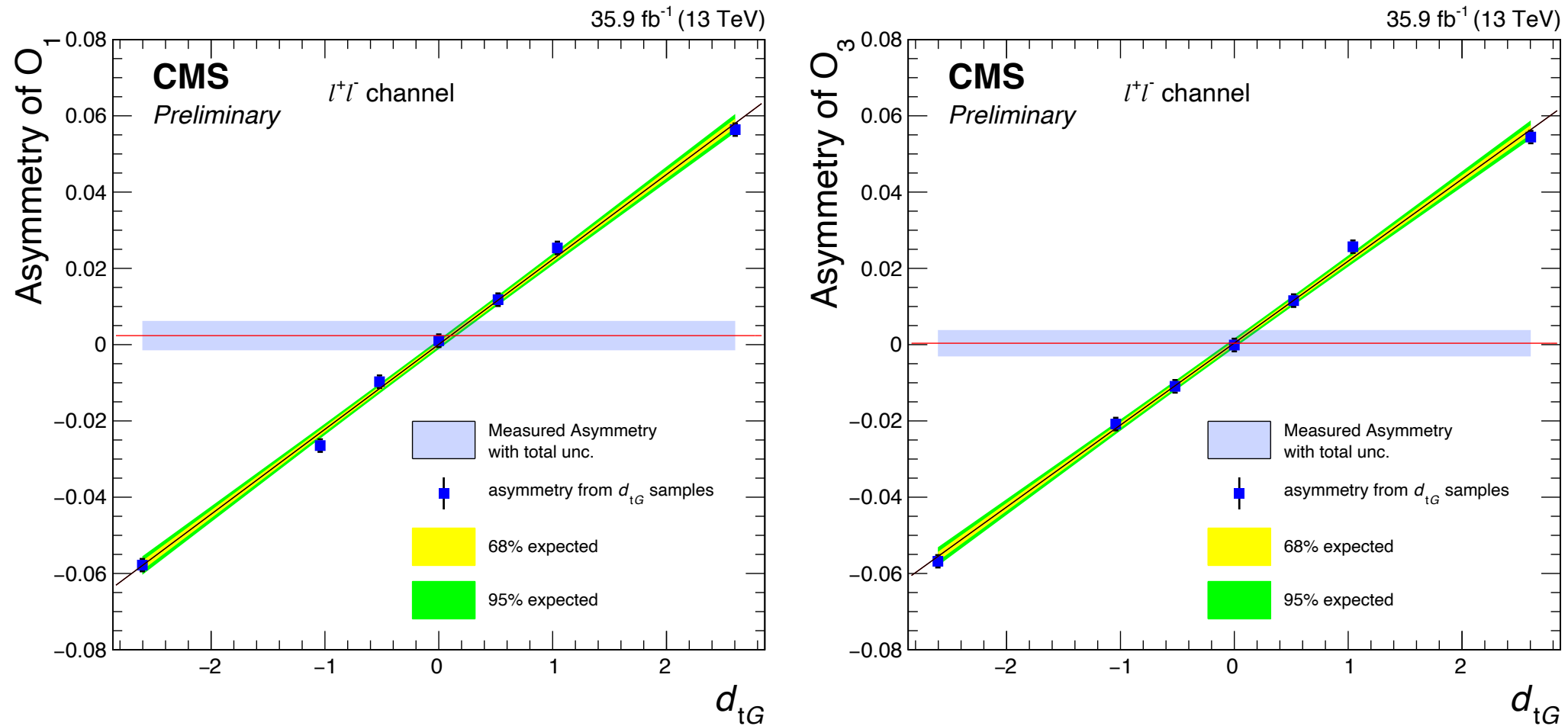


-Dominant Systematic Sources : **Color-reconnection, Underlying event**

- Asymmetry of combined channel is estimated by using best linear unbiased estimator (BLUE) method
- The measured asymmetries are consistent with the Standard Model prediction** within statistical and systematical uncertainties

Extraction of CEDM

- Asymmetry and CEDM have linear correlation



- CEDM is extracted by exploiting its correlation with the asymmetry
 $-Asymmetry = a \cdot d_{tG} + b$; using the linear fit result, we can extract the CEDM

Physics observable	d_{tG}	CEDM ($10^{-18} g_s \cdot cm$)
\mathcal{O}_1	$0.10 \pm 0.12(\text{stat}) \pm 0.12(\text{syst})$	$0.58 \pm 0.69(\text{stat}) \pm 0.70(\text{syst})$
\mathcal{O}_3	$-0.00 \pm 0.13(\text{stat}) \pm 0.10(\text{syst})$	$-0.01 \pm 0.72(\text{stat}) \pm 0.58(\text{syst})$

- The CEDMs we extracted are consistent with the SM prediction

Summary & Plan

- CP violating asymmetries and CEDM of top quark have been presented
- 2016 data set (CMS, 35.9 fb⁻¹) was analyzed
- Measured Asymmetries for combined channel are
 $2.4 \pm 2.8(\text{stat}) \pm 2.8(\text{syst}) \times 10^{-3}$ and $0.4 \pm 2.8(\text{stat}) \pm 2.2(\text{syst}) \times 10^{-3}$
- Measured CEDMs are $0.58 \pm 0.69(\text{stat}) \pm 0.70(\text{syst}) \times 10^{-18} g_s \cdot \text{cm}$ and
 $-0.01 \pm 0.72(\text{stat}) \pm 0.58(\text{syst}) \times 10^{-18} g_s \cdot \text{cm}$
- Measured asymmetries and CEDM are consistent with the Standard Model prediction within uncertainties
- We have a plan for using Run 2 Full data set



Backup

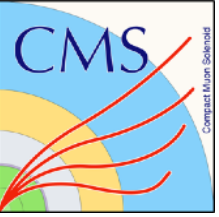


TABLE I. Comparison of asymmetries in the dilepton and semileptonic channels for $d_{tG} = 3$, $\Lambda = 1$ TeV. The latter do not yet correspond to observable asymmetries and serve only for this comparison.

	$pp \rightarrow t\bar{t} \rightarrow b\bar{b}\ell^+\ell^- E_T$	$pp \rightarrow t\bar{t} \rightarrow b\bar{b}\ell^\pm jj E_T$
\mathcal{O}_1	$\epsilon(t, \bar{t}, \ell^+, \ell^-)$	$q_\ell \epsilon(t, \bar{t}, \ell, d)$
A_1	-0.1540	$-0.1535 \xrightarrow{P_{t \rightarrow P_{t-vis}}} -0.1114$
\mathcal{O}_2	$\epsilon(t, \bar{t}, b, \bar{b})$	$\epsilon(t, \bar{t}, b, \bar{b})$
A_2	-0.0358	$-0.0311 \xrightarrow{P_{t \rightarrow P_{t-vis}}} -0.0527$
\mathcal{O}_3	$\epsilon(b, \bar{b}, \ell^+, \ell^-)$	$q_\ell \epsilon(b, \bar{b}, \ell, d)$
A_3	-0.0902	-0.0838
\mathcal{O}_4	$\epsilon(b^+, b^-, \ell^+, \ell^-)$	$\epsilon(b^\ell, b^d, \ell, d)$
A_4	-0.0340	-0.0319
\mathcal{O}_5	$q \cdot (\ell^+ - \ell^-) \epsilon(b, \bar{b}, \ell^+ + \ell^-, q)$	$q_\ell q \cdot \ell \epsilon(b, \bar{b}, \ell, q)$
A_5	-0.0309	-0.0115
\mathcal{O}_6	$\epsilon(P, b - \bar{b}, \ell^+, \ell^-)$	$q_\ell \epsilon(P, b - \bar{b}, \ell, d)$
A_6	0.0763	0.0742
\mathcal{O}_7	$q \cdot (t - \bar{t}) \epsilon(P, q, \ell^+, \ell^-)$	$q_\ell q \cdot (t - \bar{t}) \epsilon(P, q, \ell, d)$
A_7	-0.0373	$-0.0325 \xrightarrow{P_{t \rightarrow P_{t-vis}}} -0.0257$
\mathcal{O}_8	$q \cdot (t - \bar{t}) (P \cdot \ell^+ \epsilon(q, b, \bar{b}, \ell^-) + P \cdot \ell^- \epsilon(q, b, \bar{b}, \ell^+))$	$q \cdot (t - \bar{t}) (P \cdot \ell \epsilon(q, b, \bar{b}, d) + P \cdot d \epsilon(q, b, \bar{b}, \ell))$
A_8	0.0074	$0.0113 \xrightarrow{P_{t \rightarrow P_{t-vis}}} 0.0094$
\mathcal{O}_9	$q \cdot (\ell^+ - \ell^-) \epsilon(b + \bar{b}, q, \ell^+, \ell^-)$	$q \cdot \ell \epsilon(b + \bar{b}, q, \ell, d)$
A_9	0.0089	0.0051
\mathcal{O}_{10}	$q \cdot (b - \bar{b}) \epsilon(b, \bar{b}, q, \ell^+ + \ell^-)$	$q \cdot (b - \bar{b}) \epsilon(b, \bar{b}, q, d)$
A_{10}	-0.0069	-0.0045
\mathcal{O}_{11}	$q \cdot (b - \bar{b}) \epsilon(P, q, b + \bar{b}, \ell^+ - \ell^-)$	$q_\ell q \cdot (b - \bar{b}) \epsilon(P, q, b + \bar{b}, d)$
A_{11}	-0.0147	0.0140
\mathcal{O}_{12}	$q \cdot (b - \bar{b}) \epsilon(P, q, b, \bar{b})$	$q \cdot (b - \bar{b}) \epsilon(P, q, b, \bar{b})$
A_{12}	0.0058	0.0041
\mathcal{O}_{13}	$\epsilon(P, b + \bar{b}, \ell^+, \ell^-)$	$q_\ell \epsilon(P, b + \bar{b}, \ell, d)$
A_{13}	0.0032	0.0025

\mathcal{O}_1 and \mathcal{O}_3 are described in this theory paper.[1]

According to theory paper, \mathcal{O}_1 and \mathcal{O}_3 are very sensitive.

[1] <https://journals.aps.org/prd/pdf/10.1103/PhysRevD.93.014020>

- MET Filters :
 - Primary vertex filter
 - Beam halo filter
 - HBHE noise filter
 - HBHEiso noise filter
 - ee badSC noise filter (Applied only to data)
 - badMuon filter
 - badCharged hadron filter

- Triggers

	Data	MC
$\mu\mu$	HLT_IsoMu24_v*, HLT_IsoTrkMu24_v* (B to H) HLT_Mu17_TrkIsoVVL_Mu8_TrkIsoVVL_v*, HLT_Mu17_TrkIsoVVL_TkMu8_TrkIsoVVL_v* (B to G) HLT_Mu17_TrkIsoVVL_Mu8_TrkIsoVVL_DZ_v*, HLT_Mu17_TrkIsoVVL_TkMu8_TrkIsoVVL_DZ_v* (H)	HLT_IsoMu24_v*, HLT_IsoTkMu24_v*, HLT_Mu17_TrkIsoVVL_Mu8_TrkIsoVVL_v*, HLT_Mu17_TrkIsoVVL_TkMu8_TrkIsoVVL_v*
ee	HLT_Ele27_WPTight_Gsf_v*, HLT_Ele23_Ele12_CaloIdL_TrackIdL_IsoVL_DZ_v* (B to H)	HLT_Ele27_WPTight_Gsf_v* HLT_Ele23_Ele12_CaloIdL_TrackIdL_IsoVL_DZ_v*
$e\mu$	HLT_IsoMu24_v*, HLT_IsoTkMu24_v*, HLT_Ele27_WPTight_Gsf_v* (B to H) HLT_Mu23_TrkIsoVVL_Ele12_CaloIdL_TrackIdL_IsoVL_v*, HLT_Mu8_TrkIsoVVL_Ele23_CaloIdL_TrackIdL_IsoVL_v* (B to G) HLT_Mu23_TrkIsoVVL_Ele12_CaloIdL_TrackIdL_IsoVL_DZ_v*, HLT_Mu8_TrkIsoVVL_Ele23_CaloIdL_TrackIdL_IsoVL_DZ_v* (H)	HLT_IsoMu24_v*, HLT_IsoTkMu24_v*, HLT_Ele27_WPTight_Gsf_v*, HLT_Mu23_TrkIsoVVL_Ele12_CaloIdL_TrackIdL_IsoVL_v*, HLT_Mu8_TrkIsoVVL_Ele23_CaloIdL_TrackIdL_IsoVL_v*



Configuration & Setup



- CMSSW version : **CMSSW_8_0_26_patch1** • Lumi : **35.9 fb⁻¹**
- Global Tag : 80X_dataRun2_2016SeptRepro_v7(DATA)
80X_mcRun2_asymptotic_2016_TracheIV_v8(MC)
- Json : **Official Golden** (Cert 271036-284044_13TeV_23Sep2016ReReco_Collisions16_JSON)

- **Data Sets**

Channel	Data Set
Dimuon	Single(Double)Muon/Run2016(B-H)-03Feb2017*/MINIAOD
Dielectron	SingleElectron(DoubleEG)/Run2016(B-H)-03Feb2017 ver2-v2/MINIAOD
Muon-Electron	SingleMuon(Electron)/Run2016(B-H)-03Feb2017*/MINIAOD MuonEG/Run2016(B-H)-03Feb2017*/MINIAOD

- **MC Samples :**

	Sample name
TTJets	/TT_TuneCUETP8M2T4_13TeV-powheg-pythia8/RunIISummer16MiniAODv2-PUMoriond17_(backup)_80X_mcRun2_asymptotic_2016_TracheIV_v6-v1
DY 10to50	/DYJetsToLL_M-10to50_TuneCUETP8M1_13TeV-madgraphMLM-pythia8/RunIISummer16MiniAODv2-PUMoriond17_80X_mcRun2_asymptotic_2016_TracheIV_v6(ext1)-v1/
DY 50	/DYJetsToLL_M-50_TuneCUETP8M1_13TeV-madgraphMLM-pythia8/RunIISummer16MiniAODv2-PUMoriond17_80X_mcRun2_asymptotic_2016_TracheIV_v6_ext1-v2/
WW	/WW_TuneCUETP8M1_13TeV-pythia8/RunIISummer16MiniAODv2-PUMoriond17_80X_mcRun2_asymptotic_2016_TracheIV_v6-(ext1)-v1/
WZ	/WZ_TuneCUETP8M1_13TeV-pythia8/RunIISummer16MiniAODv2-PUMoriond17_80X_mcRun2_asymptotic_2016_TracheIV_v6-(ext1)-v1/
ZZ	/WZ_TuneCUETP8M1_13TeV-pythia8/RunIISummer16MiniAODv2-PUMoriond17_80X_mcRun2_asymptotic_2016_TracheIV_v6-(ext1)-v1/
ST_tW_top	/ST_tW_top_5f_inclusiveDecays_13TeV-powheg-pythia8_TuneCUETP8M1/RunIISummer16MiniAODv2-PUMoriond17_80X_mcRun2_asymptotic_2016_TracheIV_v6_ext1-v1
ST_tW_antitop	/ST_tW_antitop_5f_inclusiveDecays_13TeV-powheg-pythia8_TuneCUETP8M1/RunIISummer16MiniAODv2-PUMoriond17_80X_mcRun2_asymptotic_2016_TracheIV_v6_ext1-v1/
TTbar_WJetToLNu	/TTWJetsToLNu_TuneCUETP8M1_13TeV-amcatnloFXFX-madspin-pythia8/RunIISummer16MiniAODv2-PUMoriond17_80X_mcRun2_asymptotic_2016_TracheIV_v6_ext1-v3/MINIAODSIM
TTbar_WQQ	/TTWJetsToQQ_TuneCUETP8M1_13TeV-amcatnloFXFX-madspin-pythia8/RunIISummer16MiniAODv2-PUMoriond17_80X_mcRun2_asymptotic_2016_TracheIV_v6-v1/MINIAODSIM
TTbar_ZToLLNuNu	/TTZToLLNuNu_M-10_TuneCUETP8M1_13TeV-amcatnlo-pythia8/RunIISummer16MiniAODv2-PUMoriond17_80X_mcRun2_asymptotic_2016_TracheIV_v6_ext1-v1/MINIAODSIM
TTbar_ZQQ	/TTZToQQ_TuneCUETP8M1_13TeV-amcatnlo-pythia8/RunIISummer16MiniAODv2-PUMoriond17_80X_mcRun2_asymptotic_2016_TracheIV_v6-v1/MINIAODSIM

- To determine DY background, we've follow the method which was suggested in [1,2,3].
- For the estimation of DY background outside the dilepton invariant mass window ($76 < M_{ll} < 106 \text{ GeV}/c^2$) in data, **it is necessary to derive the ratio of DY events outside to inside the dilepton invariant mass window, $R_{out/in}$.**

$$N_{out}^{l^+l^-}, data = R_{out/in}^{l^+l^-} (N_{in}^{l^+l^-}, data - 0.5 \cdot k_{ll} \cdot N_{in}^{e\mu}, data)$$

where $ll = \mu\mu$ or ee , $R_{out/in} = \frac{N_{DY MC}^{out}}{N_{DY MC}^{in}}$ for k_{ll} , $k_{ee} = \sqrt{\frac{N_{in}^{e^+e^-}}{N_{out}^{\mu^+\mu^-}}}$, $k_{\mu\mu} = \sqrt{\frac{N_{in}^{\mu^+\mu^-}}{N_{out}^{e^+e^-}}}$

	$\mu^+\mu^-$	e^+e^-	$e^\pm\mu^\mp$
SF	1.1	1.1	1.2

[1]E. P. J. Cuevas, J. R. Gonzalez, "Measurement of the Top-Quark Pair Production Cross Section in the Dilepton Channel with 35.9 fb⁻¹ of 13 TeV data using the Cut and Count Method", CMS Note 2017/039, 2017
 [2]W. Andrews and et al., "A Method to Measure the Contribution of DY → l+l- to a di-lepton + MET Selection", CMS Note 2009/023, 2009.
 [3]S. Chenarani and et al., "Measurement of the cross-section for tW production in dilepton final states at 13 TeV using 2016 data", CMS Note 2017/132, 2017.

- There are eight equations describing the kinematics of ttbar dilepton events.

$$\begin{aligned} E_x &= p_{\nu_x} + p_{\bar{\nu}_x} \\ E_y &= p_{\nu_y} + p_{\bar{\nu}_y} \\ E_\nu^2 &= p_{\nu_x}^2 + p_{\nu_y}^2 + p_{\nu_z}^2 + m_\nu^2 \\ E_{\bar{\nu}}^2 &= p_{\bar{\nu}_x}^2 + p_{\bar{\nu}_y}^2 + p_{\bar{\nu}_z}^2 + m_{\bar{\nu}}^2 \end{aligned}$$

$$\begin{aligned} m_{W^+}^2 &= (E_{\ell^+} + E_\nu)^2 - (p_{\ell_x^+} + p_{\nu_x})^2 \\ &\quad - (p_{\ell_y^+} + p_{\nu_y})^2 - (p_{\ell_z^+} + p_{\nu_z})^2 \\ m_{W^-}^2 &= (E_{\ell^-} + E_{\bar{\nu}})^2 - (p_{\ell_x^-} + p_{\bar{\nu}_x})^2 \\ &\quad - (p_{\ell_y^-} + p_{\bar{\nu}_y})^2 - (p_{\ell_z^-} + p_{\bar{\nu}_z})^2 \\ m_t^2 &= (E_b + E_{\ell^+} + E_\nu)^2 - (p_{b_x} + p_{\ell_x^+} + p_{\nu_x})^2 \\ &\quad - (p_{b_y} + p_{\ell_y^+} + p_{\nu_y})^2 - (p_{b_z} + p_{\ell_z^+} + p_{\nu_z})^2 \\ m_{\bar{t}}^2 &= (E_{\bar{b}} + E_{\ell^-} + E_{\bar{\nu}})^2 - (p_{\bar{b}_x} + p_{\ell_x^-} + p_{\bar{\nu}_x})^2 \\ &\quad - (p_{\bar{b}_y} + p_{\ell_y^-} + p_{\bar{\nu}_y})^2 - (p_{\bar{b}_z} + p_{\ell_z^-} + p_{\bar{\nu}_z})^2 \end{aligned}$$

- Details of reconstruction method

1. Input Object :

reconstructed jets, leptons, MET

2. Input to kinematic reconstruction :

- Correction for detector effects:

Jet & lepton energies smeared

- **Directional smearing**

3. Top Mass Fixed: **172.5 GeV**

4. **W mass on the reco level is smeared** according to the true W mass distribution.

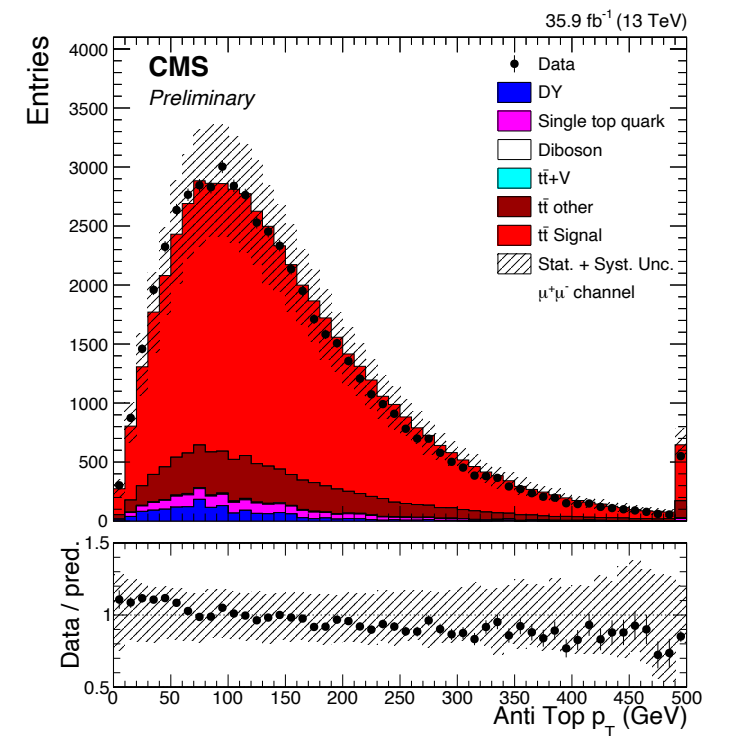
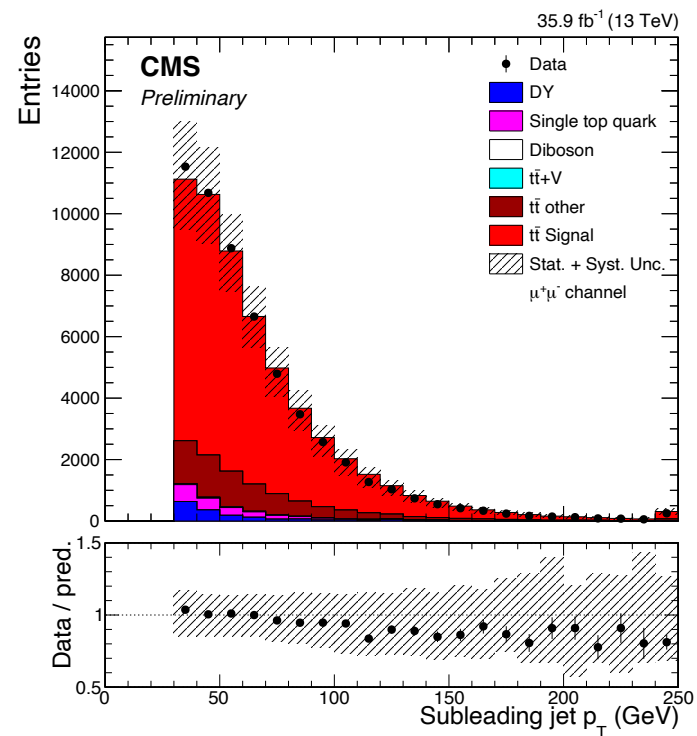
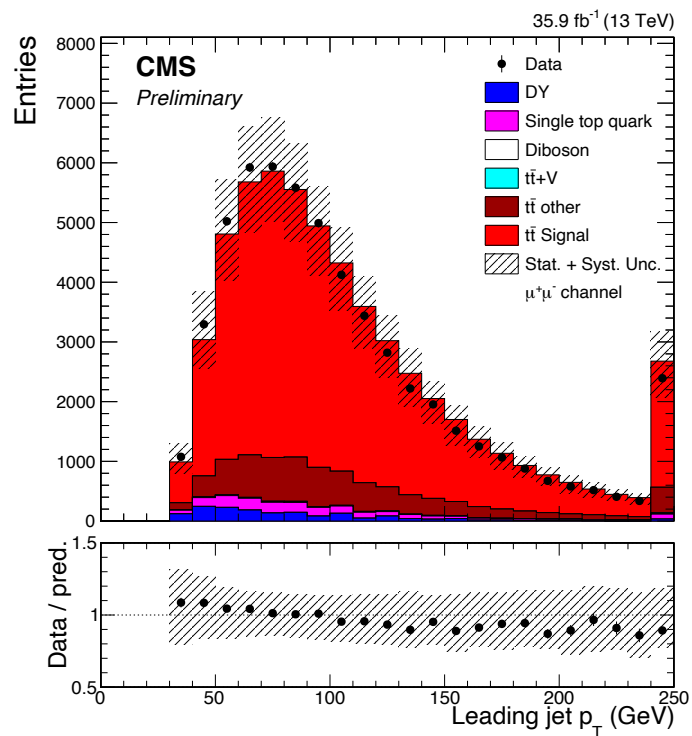
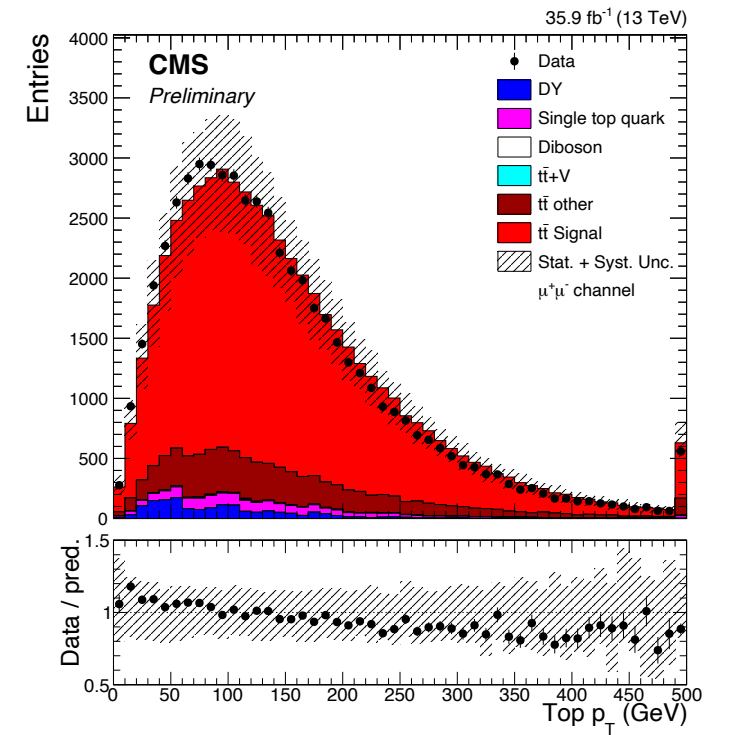
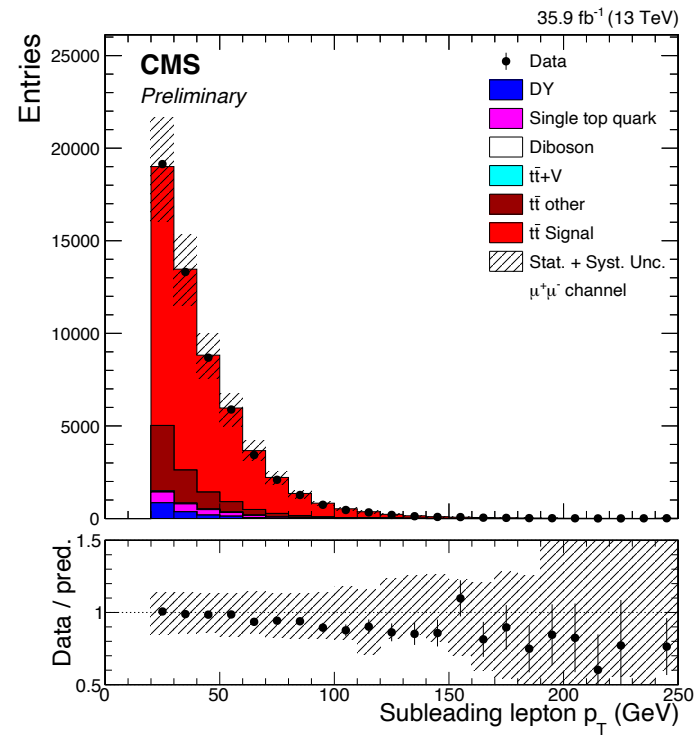
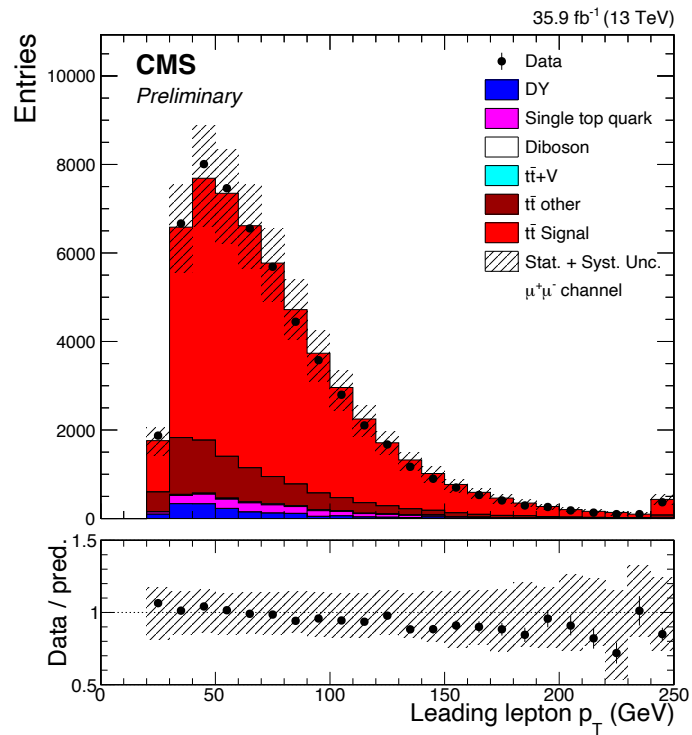
5. Combinatorics solved: **ONLY** the Lepton-Jet

combination with the largest sum of solution weights according to **true m(bl) spectrum** is taken

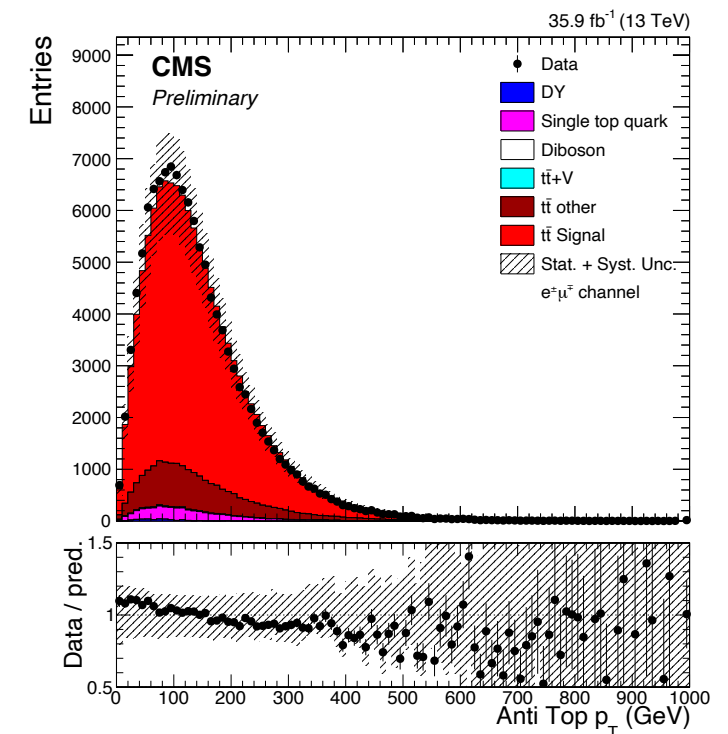
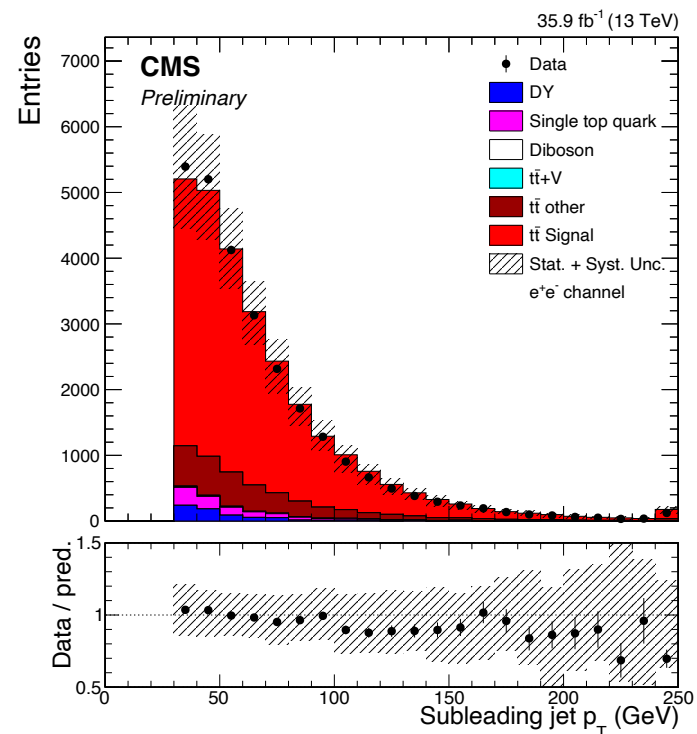
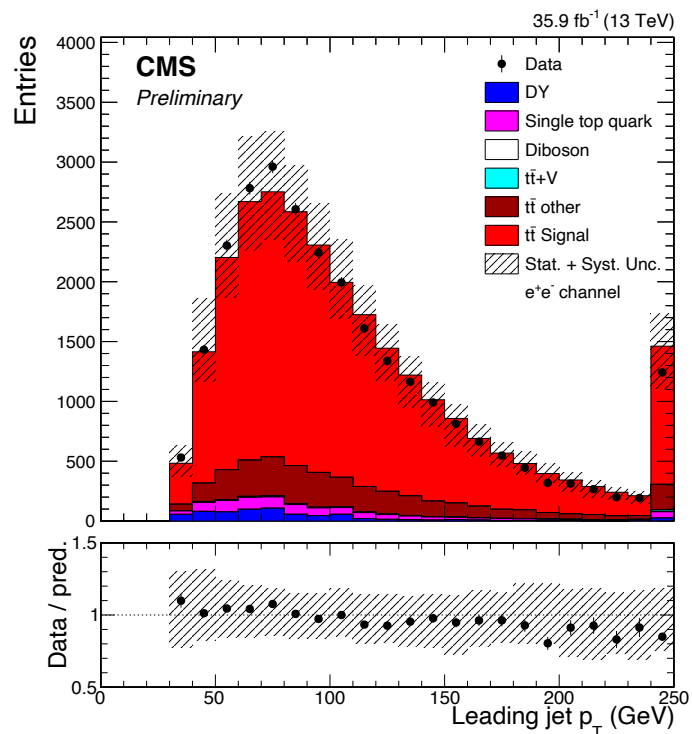
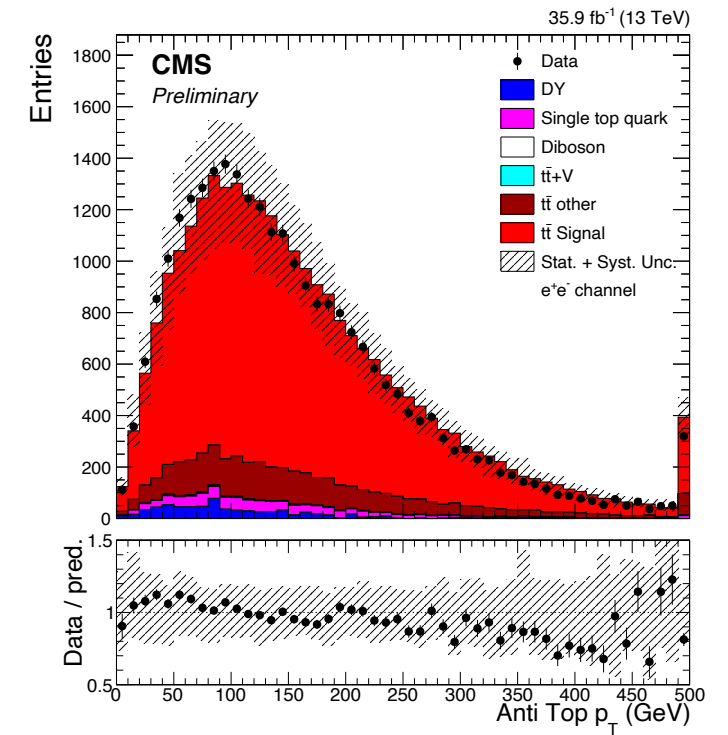
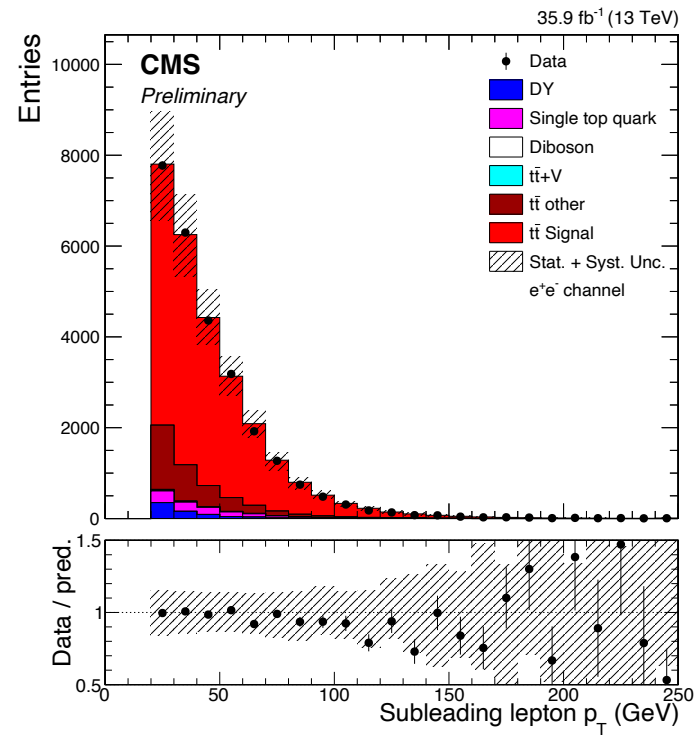
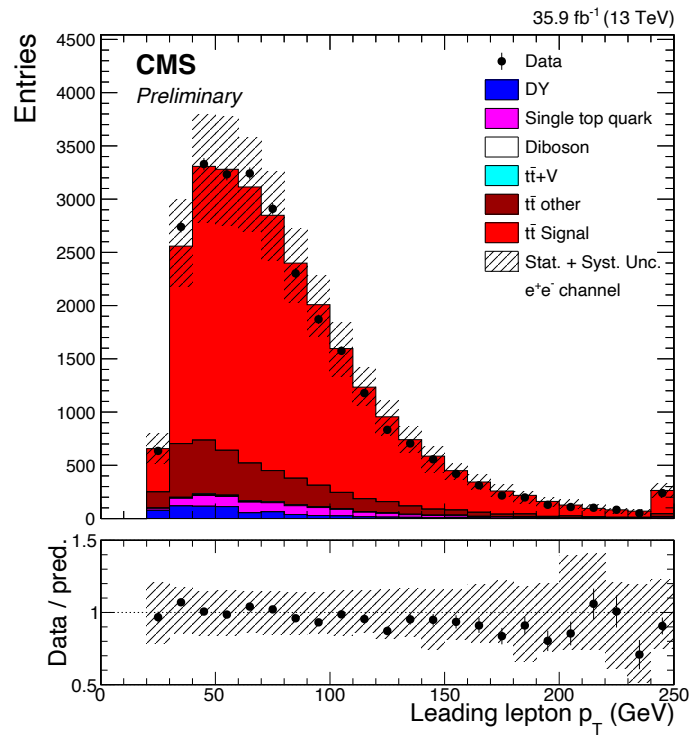
6. Solution ambiguities: solution with **smallest m(tt) is taken.**

7. weighted average solution is taken.

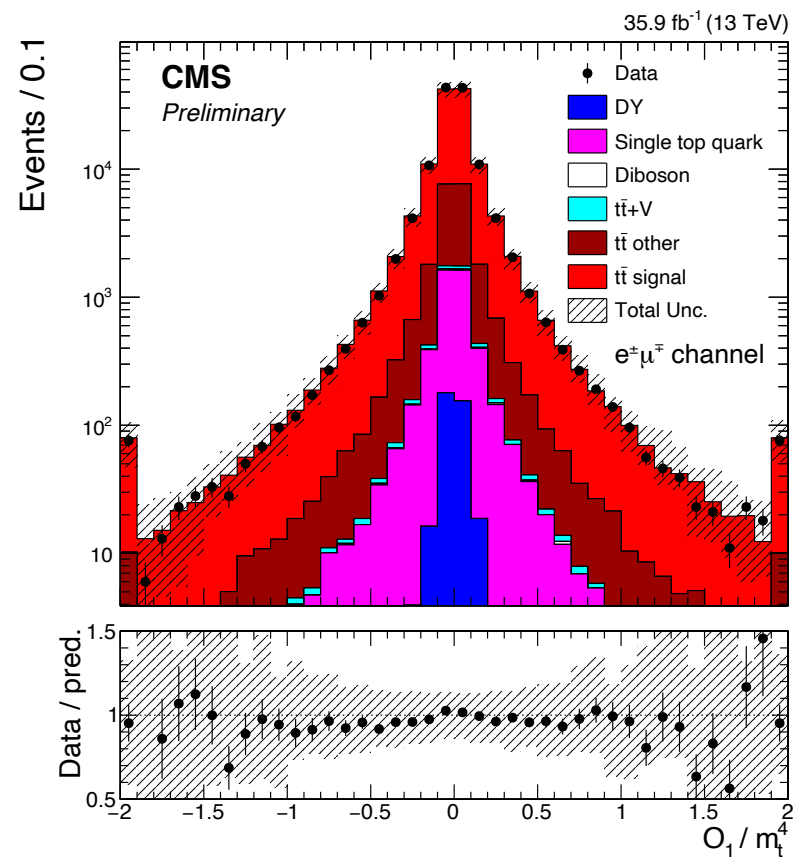
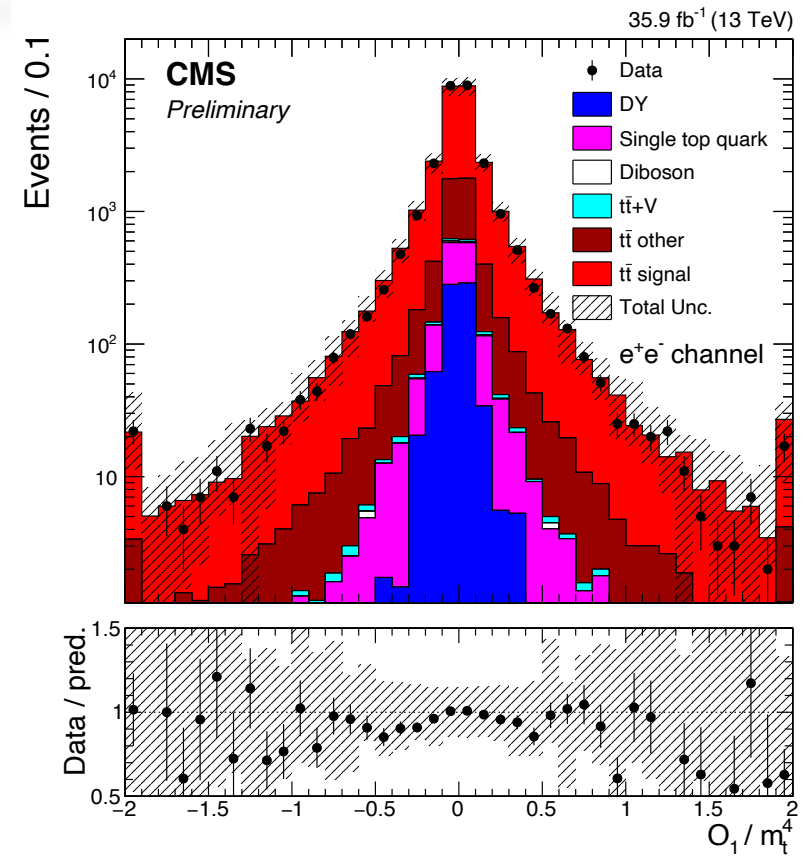
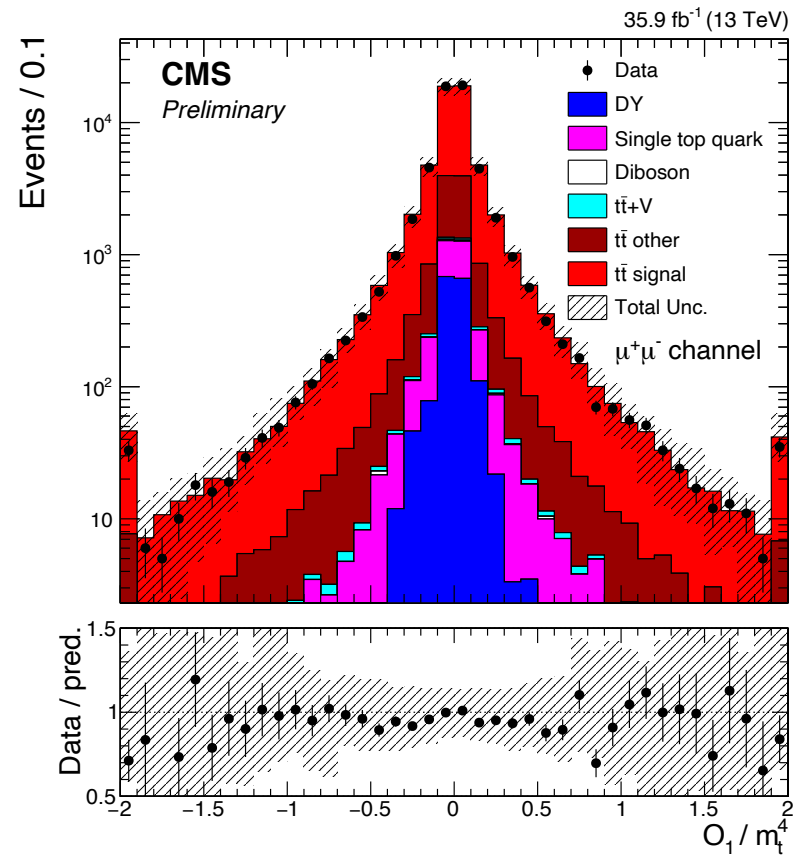
Kinematics of Object ($\mu^+ \mu^-$)



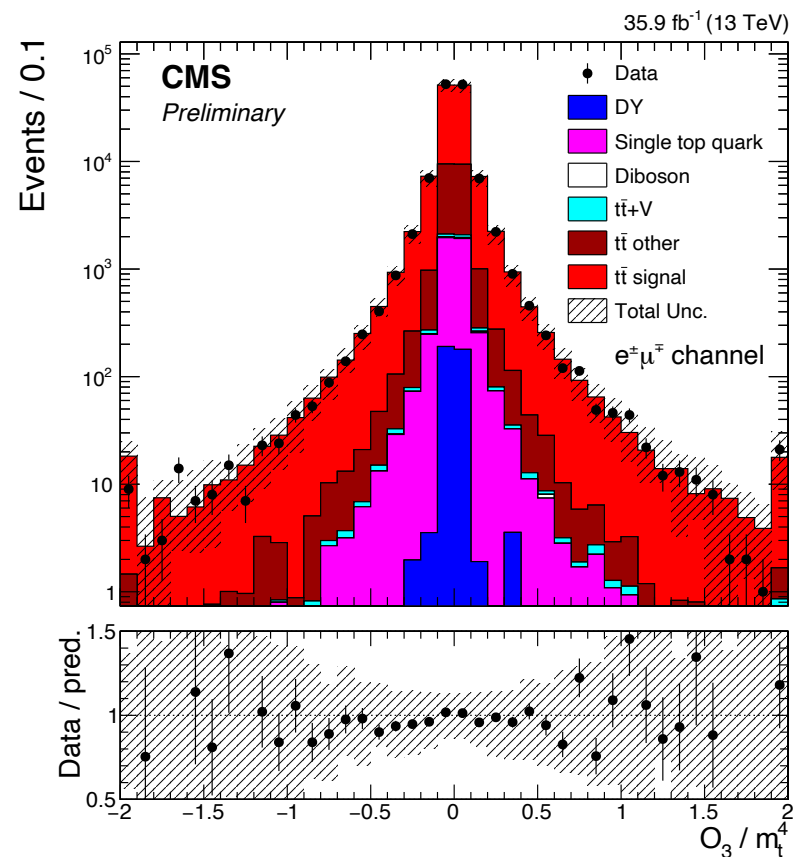
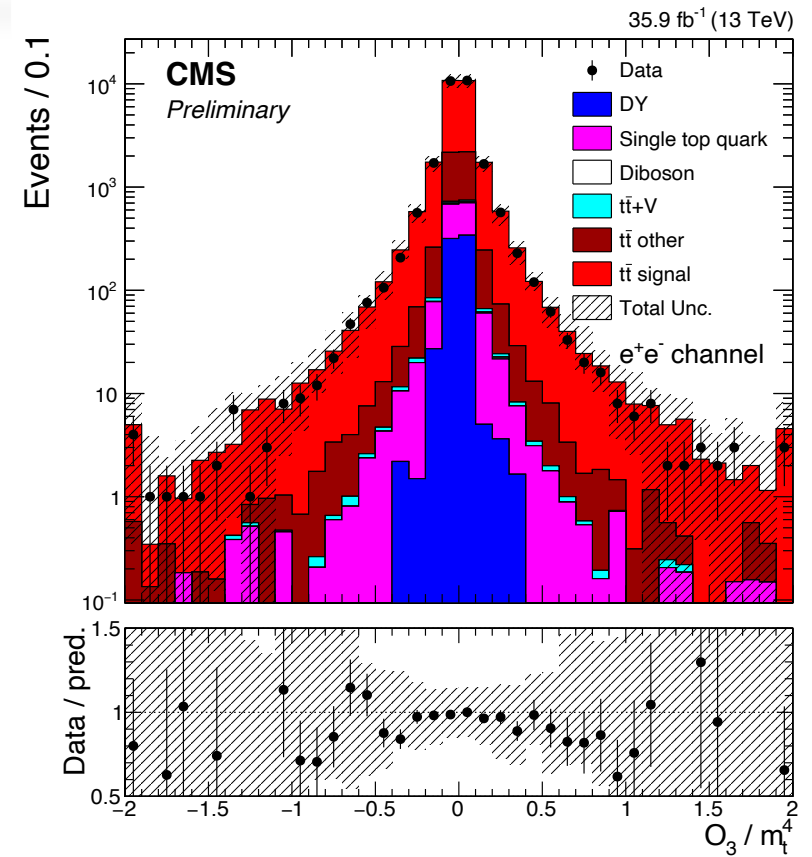
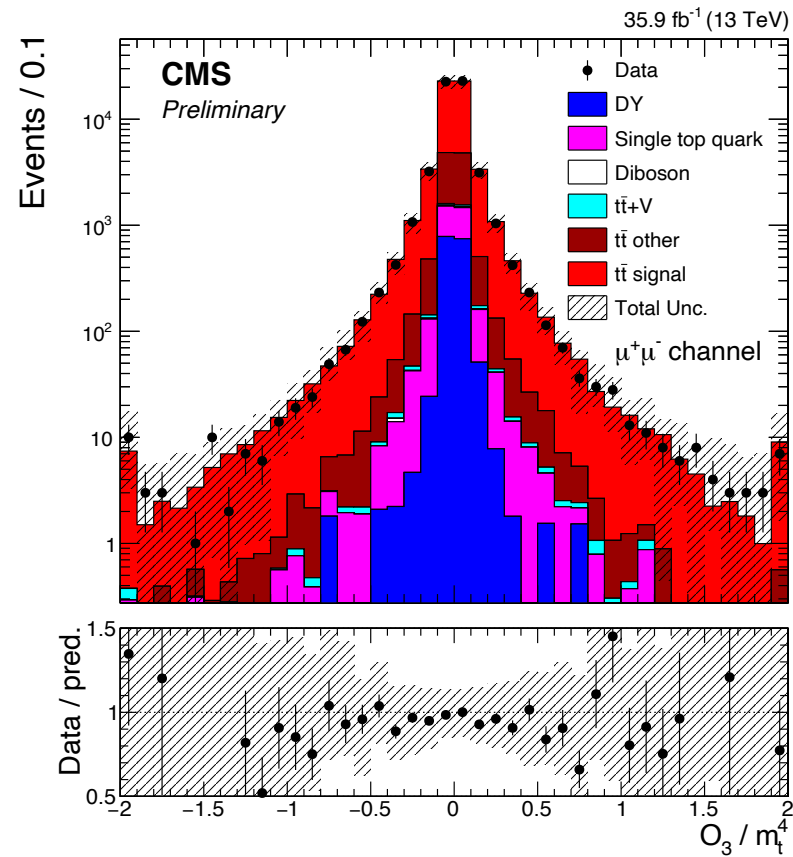
Kinematics of Object (e^+e^-)



Distribution of O_1



Distribution of O_3



For Positive Area

1. Only one mis-identified charge of lepton

(We got same sign leptons, Veto Event)

- N_p = # of events in positive Area
- f = charge mis-Id probability (Lep)
- f' = charge mis-Id probability (An-Lep)
- $P_{\text{mis-id}} = (1-f') \times f + (1-f) \times f'$
- $N_{\text{veto}} = N_p * P_{\text{mis-id}}$

$$N_p' = N_p - N_{\text{veto}}$$

$$N_{\text{total}}' = N_{\text{total}} - N_{\text{veto}}$$

2. Mis-identified charge of two leptons

(Changing sign of O_i)

- N_p = # of events in positive Area
- f = charge mis-Id probability (Lep)
- f' = charge mis-Id probability (An-Lep)
- $P_{\text{mis-id}} = f' \times f$
- $N_{p \rightarrow m} = N_p * P_{\text{mis-id}}$

$$N_p' = N_p - N_{p \rightarrow m}$$

$$N_m' = N_m + N_{p \rightarrow m}$$

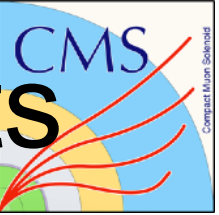
- In case of only one charge mis-identification, if one lepton charge is mis-identified, the charge of the other lepton is correctly identified. This event contains same charge of leptons, so that it is rejected. The number of vetoed events is $N_{\text{veto}} = N_p * P_{\text{mis-id}}$
- For mis-identification of the charges of two leptons, we evaluated how many events in the positive area moved to the negative area.
- We did the same procedure for negative area.

Charge Mis-Identification

Channel	Case	Uncertainty ($\times 10^{-3}$)	
		$\Delta A(O_1)$	$\Delta A(O_3)$
Dimuon	Only one charge mis-identified lepton		
	Positive area	0.1	0.1
	Negative area	-0.1	-0.1
	Two charge mis-identified lepton		
	Positive area	0.1	0.1
	Negative area	-0.1	-0.1
Dielectron	Only one charge mis-identified lepton		
	Positive area	1.0	1.0
	Negative area	-1.0	-1.0
	Two charge mis-identified lepton		
	Positive area	1.0	1.0
	Negative area	-1.0	-1.0
Muon-Electron	Only one charge mis-identified lepton		
	Positive area	0.4	0.4
	Negative area	-0.4	-0.4
	Two charge mis-identified lepton		
	Positive area	0.1	0.1
	Negative area	-0.1	-0.1



Difference Response to b and bbar-quark jets



- Our analysis can be affected by a different response of the calorimeter to quark and antiquark jets, because the four-vectors for b/b^- -quark jets participate in the contractions of the Levi-Civita tensor and the kinematic top quark reconstruction.
- K^- and K^+ mesons are the **dominant fragments of b/b^- -quarks**, which fly to the calorimeter and interact with its absorbers. Furthermore, **they have different inelastic nuclear cross sections**. As a result, **the different contents of K^- and K^+ mesons from the fragmentations of b/b^- -quarks lead the calorimeter to respond to b/b^- -quark jets differently**.
- The calorimeter responses to b/b -quark jets are modeled with no difference in MC, while such a difference is present in data.

Measured Asymmetries

Physics observable	Asymmetry and Uncertainty ($\times 10^{-3}$)			
	$\mu^+\mu^-$	e^+e^-	$e^\pm\mu^\mp$	combined channel
\mathcal{O}_1	6.9 ± 5.3	8.8 ± 7.5	0.6 ± 3.4	2.4 ± 2.8
\mathcal{O}_3	6.1 ± 5.3	4.1 ± 7.5	-1.7 ± 3.4	0.4 ± 2.8

Table 3: Systematic uncertainties of asymmetries of \mathcal{O}_1 , as detailed in the text.

Source	Uncertainty ($\times 10^{-3}$)							
	$\mu^+\mu^-$		e^+e^-		$e^\pm\mu^\mp$		Combined	
	up	down	up	down	up	down	up	down
Muon energy	2.3	-2.3	-	-	0.1	-0.1	0.5	-0.5
Electron scale and smearing	-	-	1.2	-1.2	0.2	-0.2	0.3	-0.3
JES	2.3	-2.3	1.9	-1.9	0.1	-0.1	0.7	-0.7
JER	1.2	-1.2	2.0	-2.0	0.3	-0.3	0.6	-0.6
Limited number of simulated BG events	2.3	-2.3	2.9	-2.9	0.6	-0.6	0.7	-0.7
ME-PS matching	0.8	-0.8	0.8	-0.8	0.3	-0.3	0.4	-0.4
Color reconnection	1.0	-1.0	1.9	-1.9	1.6	-1.6	1.5	-1.5
Underlying event	1.4	-1.4	0.6	-0.6	1.4	-1.4	1.4	-1.4
ISR	0.3	-0.3	1.5	-1.5	0.2	-0.2	0.3	-0.3
FSR	0.6	-0.6	1.0	-1.0	0.8	-0.8	0.7	-0.7
Hadronization	1.7	-1.7	2.0	-2.0	0.6	-0.6	0.9	-0.9
Charge misidentification	0.1	-0.1	0.8	-0.8	0.4	-0.4	0.3	-0.3
Total systematic uncertainty	5.0	-5.0	5.6	-5.6	2.6	-2.6	2.8	-2.8

Table 4: Systematic uncertainties of asymmetries of \mathcal{O}_3 , as detailed in the text.

Source	Uncertainty ($\times 10^{-3}$)							
	$\mu^+\mu^-$		e^+e^-		$e^\pm\mu^\mp$		Combined	
	up	down	up	down	up	down	up	down
Muon energy	1.0	-1.0	-	-	0.2	-0.2	0.3	-0.3
Electron scale and smearing	-	-	1.1	-1.1	0.2	-0.2	0.2	-0.2
JES	0.7	-0.7	0.6	-0.6	0.2	-0.2	0.3	-0.3
JER	0.3	-0.3	0.7	-0.7	0.2	-0.2	0.2	-0.2
Limited number of simulated BG events	2.3	-2.3	2.9	-2.9	0.6	-0.6	0.7	-0.7
ME-PS matching	1.5	-1.5	1.4	-1.4	0.7	-0.7	0.9	-0.9
Color reconnection	0.9	-0.9	3.8	-3.8	1.0	-1.0	1.1	-1.1
Underlying event	1.0	-1.0	0.9	-0.9	1.1	-1.1	1.0	-1.0
ISR	0.5	-0.5	1.8	-1.8	0.2	-0.2	0.3	-0.3
FSR	0.3	-0.3	1.9	-1.9	0.6	-0.6	0.6	-0.6
Hadronization	0.2	-0.2	0.5	-0.5	0.3	-0.3	0.3	-0.3
Charge misidentification	0.1	-0.1	0.8	-0.8	0.4	-0.4	0.3	-0.3
Total systematic uncertainty	3.5	-3.5	6.0	-6.0	2.0	-2.0	2.2	-2.2

BLUE method is used to combine the asymmetries for three channels

Limited statistics of background (BG) models

$$\mathcal{L}(A_{\mathcal{O}_i}, \sigma_{t\bar{t}}) = \prod_k \mathcal{P}(N_k^{obs}, N_k^{pred})$$

$$N_k^{pred} = N_t^{t\bar{t}} \frac{1 + A_{\mathcal{O}_i} f_k^{\mathcal{O}_i > 0}}{2} + N_t^{t\bar{t}} \frac{1 - A_{\mathcal{O}_i} f_k^{\mathcal{O}_i < 0}}{2} + N^{bkg} f_k^{bkg}$$

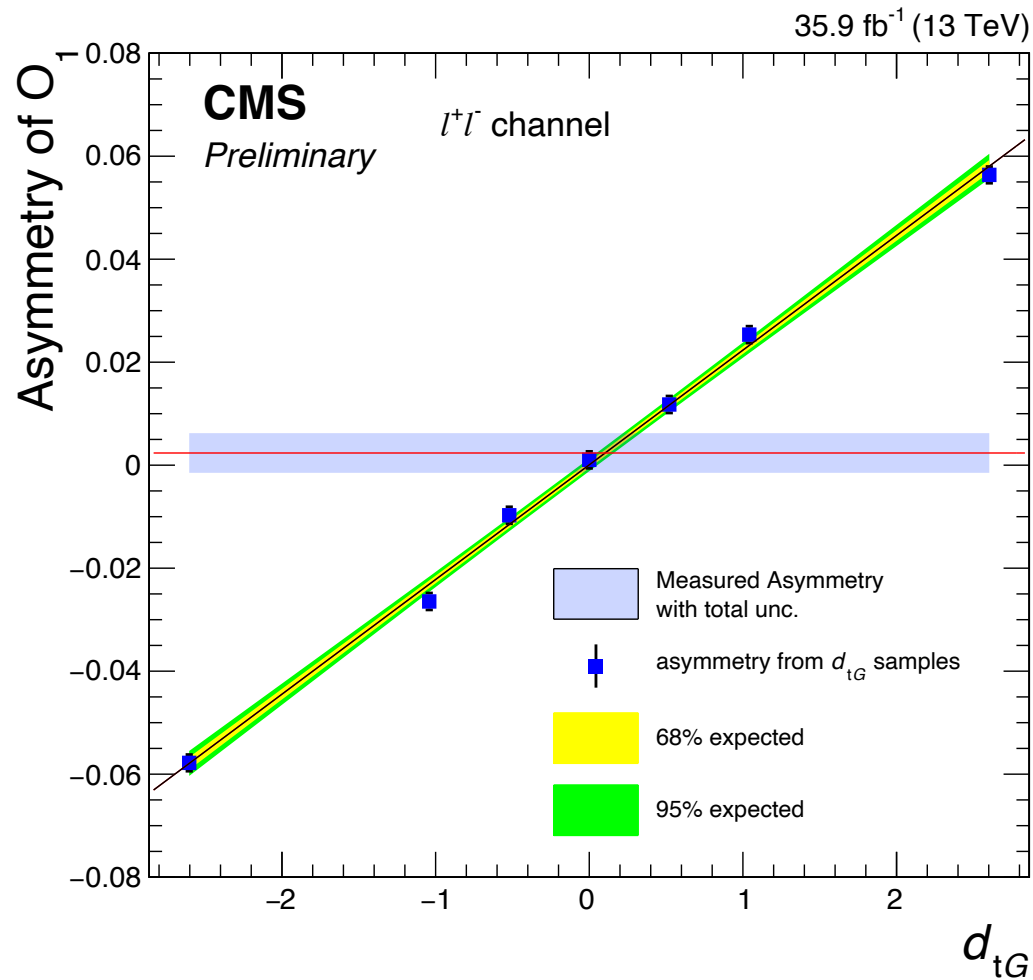
where $N_t^{t\bar{t}} = \mathcal{L} \cdot \text{Branching Ratio} \cdot \epsilon_{sig} \cdot \sigma_{t\bar{t}}$

Gaussian constraints.

$$\mathcal{L}(A_{\mathcal{O}_i}, \sigma_{t\bar{t}}) = \prod_k \mathcal{P}(N_k^{obs}, N_k^{pred}) = \prod_k \text{Pois}(N_k^{obs} | A_{\mathcal{O}_i}, \sigma_{t\bar{t}}, N_{neg}^{bkg}, N_{pos}^{bkg})$$

$$\text{Gaus}(N_{neg}^{bkg} | \mu_{neg}, \sigma_{neg}) \text{Gaus}(N_{pos}^{bkg} | \mu_{pos}, \sigma_{pos})$$

- Background Monte Carlo samples are generated with the limited numbers of events. Therefore, the total number of background events has fluctuations on the basis of the statistical uncertainty.
- The fluctuations of asymmetries by the limited statistics of background models are investigated by setting **the numbers of the background events in the negative and positive regions as the nuisance parameters.**



- We generate CP violating tt events decaying to the dilepton channels.
- These samples were generated with several d_{tG} values.

$$\text{Asymmetry} = a \cdot d_{tG} + b$$

$$d_{tG} = \frac{\text{Asymmetry} - b}{a}$$

$$\Delta_{d_{tG}}^2 = \begin{pmatrix} \frac{\partial d_{tG}}{\partial A} & \frac{\partial d_{tG}}{\partial b} & \frac{\partial d_{tG}}{\partial a} \end{pmatrix} \begin{pmatrix} \Delta_A^2 & 0 & 0 \\ 0 & \Delta_b^2 & \mathbf{COV}(b, a) \\ 0 & \mathbf{COV}(a, b) & \Delta_a^2 \end{pmatrix} \begin{pmatrix} \frac{\partial d_{tG}}{\partial A} \\ \frac{\partial d_{tG}}{\partial b} \\ \frac{\partial d_{tG}}{\partial a} \end{pmatrix}$$

a, b can be obtained from linear fitting.

TOP-18-007 (1-sigma unc.)

Obs	d_{tG}	\hat{d}_t
O1	0.103 \pm 0.175	0.006 \pm 0.011
O3	-0.002 \pm 0.163	-0.000 \pm 0.010

TOP-18-006 (95% CL.) [1]

Coupling	95% CL	Theoretical unc.	χ^2	Coefficients
$\hat{\mu}_t$	$-0.014 < \hat{\mu}_t < 0.004$	± 0.001	7	$C_{kk}, C_{nn}, C_{rk} + C_{kr}, D$
\hat{d}_t	$-0.020 < \hat{d}_t < 0.012$	—	9	$B_2^r, B_1^n, C_{nr} - C_{rn}, C_{nk} - C_{kn}$
\hat{c}_{--}	$-0.040 < \hat{c}_{--} < 0.006$	± 0.001	7	$B_2^r, B_1^n, C_{nr} - C_{rn}, C_{nk} - C_{kn}$
\hat{c}_{-+}	$-0.009 < \hat{c}_{-+} < 0.005$	—	11	$B_1^n, B_2^n, B_1^{r*}, C_{nk} + C_{kn}$
\hat{c}_{VV}	$-0.011 < \hat{c}_{VV} < 0.042$	± 0.004	7	$C_{kk}, C_{nn}, C_{rk} + C_{kr}, D$
\hat{c}_{VA}	$-0.044 < \hat{c}_{VA} < 0.027$	± 0.003	9	$B_2^k, B_2^r, C_{kk}, C_{nr} + C_{rn}$
\hat{c}_{AV}	$-0.035 < \hat{c}_{AV} < 0.032$	± 0.001	6	$B_1^{k*}, B_2^{k*}, B_1^{r*}, B_2^{r*}$
\hat{c}_1	$-0.09 < \hat{c}_1 < 0.34$	± 0.04	7	$C_{kk}, C_{nn}, C_{rk} + C_{kr}, D$
\hat{c}_3	$-0.35 < \hat{c}_3 < 0.21$	± 0.02	9	$B_2^k, B_2^r, C_{kk}, C_{nr} + C_{rn}$
$\hat{c}_1 - \hat{c}_2 + \hat{c}_3$	$-0.17 < \hat{c}_1 - \hat{c}_2 + \hat{c}_3 < 0.15$	± 0.01	6	$B_1^{k*}, B_2^{k*}, B_1^{r*}, B_2^{r*}$

TOP-18-007 (95% CL.)

CADI	(Observable)	\hat{d}_t
TOP-18-007	O1	$-0.014 < \hat{d}_t < 0.027$
	O3	$-0.019 < \hat{d}_t < 0.019$

CADI	\hat{d}_t
TOP-18-006	$-0.020 < \hat{d}_t < 0.012$

Our results are consistent with TOP-18-006.

Our Intervals of \hat{d}_t are larger than TOP-18-006 (about 20~30%).

[1] <http://dx.doi.org/10.1103/PhysRevD.100.072002>